Spring 5-14-2016

Characterization of a Mitochondrial Localizing Molluscum Contagiosum Virus Protein: MC163R

Jesse Coutu
jesse.coutu@student.shu.edu

Characterization of a Mitochondrial Localizing Molluscum Contagiosum Virus Protein: MC163R

By

Jesse Coutu

Submitted in partial fulfillment of the requirements for the degree of Master of Sciences in Biology from the Department of Biological Sciences of Seton Hall University May 2016

Seton Hall University

Department of Biological Sciences

APPROVED BY

MENTOR

Dr. Daniel B. Nichols

COMMITTEE MEMBER

Dr. Constantine Bitsaktsis

COMMITTEE MEMBER

Dr. Angela Klaus

DIRECTOR OF GRADUATE STUDIES

Dr. Angela Klaus

CHAIRPERSON, DEPARTMENT OF BIOLOGICAL SCIENCES

Dr. Jane Ko

Table of Contents

List of Tables

List of Figures

Acknowledgements

Dr. Daniel Brian Nichols

Friends and Family

Dr. Joanna Shisler, Guidance and support

Dr Joachim Bugert, Genomic MCV library

Abstract

Molluscum Contagiosum Virus (MCV) is an obligate human, tumorigenic poxvirus which causes benign skin neoplasms. Reduced inflammation during an MCV infection has been attributed to production of MCV immune evasion molecules (IEMs). IEMs antagonize host immune responses allowing MCV to evade the host immune system and reprogram the host cell for viral growth. MCV IEMs alter apoptosis (MC159, MC160), deregulate the cell cycle targeting retinoblastoma (MC007), and produce a chemokine homolog (MC148). Bioinformatics analysis identified MC163, as another potential host-interacting protein. Further analysis of MC163 resulted in the identification of a mitochondrial localization sequence, putative superoxide dismutase (SOD)-like Cu^{2+}/Zn^{2+} metal binding domain, a transmembrane domain and a large C-terminal domain that contains no identified homology to other viral or host proteins. Confocal microscopy was utilized to verify the predicted mitochondrial localization. MC163 was detected at the mitochondria, whereas a truncated MC163 lacking the mitochondria localization sequence was diffused throughout the cell. Mitochondria are important moderators in apoptotic and anti-viral signaling. Many viral proteins that localize to the mitochondria affect mitochondria immune signaling pathways such as apoptosis. Preliminary data suggests that expression of MC163 inhibits TNF-induced mitochondrial membrane permeabilization MMP. Therefore, MC163 expression may contribute to MCV immune evasion by antagonizing apoptotic signaling events.

Introduction

Molluscum Contagiosum Virus (MCV), a member of the *Poxviridae* family, causes benign skin lesions characterized by reduced inflammation. MCV lesions persist for months in otherwise healthy individuals. MCV lesions are spread by skin to skin contact, fomites, or autoinoculation and are most prevalent in children and immune compromised individuals, such as those with HIV (Koning et al. 1994; Tyring 2003; Mohammedamin et al. 2006). Although MCV infection is non-lethal, it causes scarring and disfigurement which can result in emotional damage, especially in children. MCV affects 2-10% of the world population and can account for 1% of the skin disorders in the United States with a higher percent in children (5%) and those infected with Human immunodeficiency virus (HIV) (5-18%) (Guan et al. 2014; Sherwani et al. 2012).

With the eradication of Smallpox, MCV remains the only poxvirus that exclusively infects humans. In 2010, 122 million cases of MCV infection were reported, highlighting the importance in understanding MCV infection and the development of effective treatment strategies. Currently, there are no antiviral treatments specific for MCV. Anti-MCV strategies rely primarily on mechanical means of removal such as curettage and cryotherapy. However, these strategies are extremely painful for patients suffering from chronic MCV infection and can result in suffering and anxiety, with limited success rates. Cidofovir is available as a drug of last resort, but off target affects limit its wide-spread use. Therefore, identification of novel anti-MCV strategies should remain a top research priority. Unfortunately, research on MCV is hampered due to the

inability to propagate MCV in cell culture or an animal model as well as a lack of understanding basic MCV-host interactions.

The *Poxviridae* family possess large, linear dsDNA genomes. Unlike most DNA viruses, poxviruses replicate exclusively in the cytoplasm of host cells. Therefore, to replicate and transcribe the viral genome, members of the poxvirus family must encode their own replication and transcription machinery. Further, by replicating inside the cytoplasm of host cells, poxviruses are exposed to a multitude of cellular innate immune responses (IIRs) that recognize and respond to viral infection. To combat innate immune defenses, poxviruses devote a substantial portion of their genome to code for a variety of host interacting proteins to modulate of cellular IIRs, such as apoptosis (Haller et al. 2014). Given that MCV persists for months in otherwise healthy individuals, it seems reasonable to speculate that like other poxviruses, MCV must possess a myriad of strategies to dampen host IIRs to sustain a persistent infection. Analysis of the MCV genome revealed that MCV encodes approximately 182 proteins, 77 of which are potential host-interacting proteins (Senkevich, et al. 1997). However, MCV host defense strategies are extremely understudied. Of these 77 predicted host-interacting molecules, only 7 have been characterized for function in host signal pathways. The 7 immune modulating proteins of MCV that have been characterized are MC007, MC054, MC066, MC132, MC148, MC159, and MC160. MC007 is a mitochondrial localizing protein that sequesters the retinoblastoma protein (pRb) (Mohr et al. 2008). MC054 is involved in binding Interlukin-18 (IL-18) blocking the pro-inflammatory cytokines function in innate and adaptive immunity (Xiang et al. 2003). MC066 is a putative glutathione peroxidase

that blocks apoptosis induced by ultraviolet light and hydrogen peroxide (Shisler et al. 1998). MC132 inhibits NF-κB activation by interaction with the p65 subunit and causes p65 degradation (Brady et al. 2015). MC148 functions as a chemokine-like protein binding to CxC12a and CCR8 and blocks chemotaxis (Jin et al. 2011; Luttichau et al. 2001). MC159 inhibits Tumor Necrosis factor-α (TNF-α), Fas, and TRAIL-induced apoptosis and blocks activation of Nuclear Factor kappa B (NF-κB) (Murao & Shisler 2005; Randall et al. 2012, Struzik et al. 2014). MC160 binds Heat Shock protein 90 and induces I kappa Kinase (IKK) degradation resulting in the inhibition of TNF-α-induced NF-κB activation (Nichols & Shisler 2006; Nichols & Shisler 2009). In this study we present evidence for a role of another MCV host-interaction protein, MC163R.

Apoptosis is a powerful antiviral response. Apoptosis can be triggered by both extrinsic and intrinsic mechanisms. The extrinsic pathway is activated by binding of ligands such as Fas Ligand (FasL), TNF-α and TNF-related apoptosis inducing ligand (TRAIL) to their respective receptors inducing a signal cascade that leads to the activation of caspases and the pro-inflammatory transcription factor NF-κB (Green & Llambi 2015).

Tumor necrosis factor-alpha (TNF-α) is a pro-inflammatory cytokine produced in response to a viral infection. Binding of TNF-α to its receptor can result in multiple responses. One outcome is the activation of the host Nuclear Factor-kappa B (NF-κB) transcription factor, which leads to the transcriptional activation of NF-κB regulated genes. Once bound to the TNF R1 receptor, TNF induces the formation of a signal complex comprised of TNF-R-associated death domain protein (TRADD), TNF-R-

associated factor 2 (TRAF2), and receptor-interacting protein 1 (RIP1) (Li & Lin. 2007). Subsequent recruitment of the I kappa Kinase (IKK) complex to the receptor complex and activation of the IKKα and IKKβ subunits causes the phosphorylation of inhibitor of kappa B alpha (IκBα) one of the NF-κB inhibitory proteins (Chen et al. 1995; DiDonato et al. 1997). Ubiquitination-dependent degradation of IκBα leads to its dissociation from NF-κB and allows for transcription of NF-κB regulated genes resulting in the transcription of pro-inflammatory mediators such as IL-6 (Li & Lin. 2007).

Alternatively, apoptosis can be induced through TNF-α signaling through TNF-R1 activation. Recruitment of the death-inducing signal complex (DISC) including TRADD, RIP1 and Fas-associated death domain (FADD) leads to the recruitment of pro-caspase 8 and activation to its active form, caspase 8 (Micheau & Tschopp 2003). Caspase 8 leads to the activation of the intrinsic apoptosis pathway through the cleavage of BH3 interacting-domain death agonist (Bid) and activation of effector caspases 3 and 7 (Elmore et al. 2013). Additionally, caspase 8 can directly activate a caspase cascade by activating effector caspases 3 and 7 (Kiraz et al. 2015). A summary of the TNF-α signaling pathway can be found in figure 1.

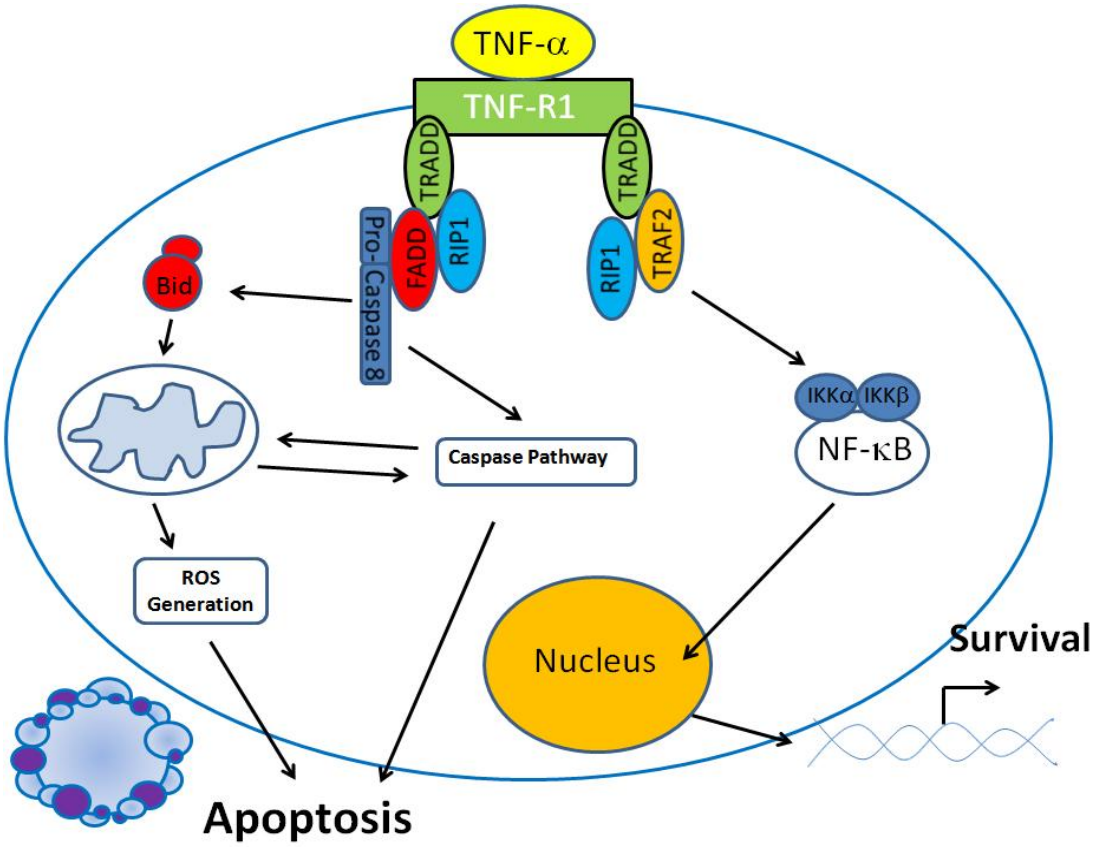

Figure 1: Tumor necrosis factor alpha (TNF-α) Signal Pathway. Activation of the TNF-α-induced response occurs after TNF-α binds its receptor. Recruitment of TRADD, TRAF2 and RIP1 to the TNF-receptor lead to activation of NF-κB and promote cell survival and inflammation, whereas, recruitment of the TRADD, FADD, RIP1 and procaspase 8 lead to apoptosis. TNF-α, tumor necrosis factor alpha; TNF-R1, TNF-receptor 1; TRADD, TNF-associated death domain; TRAF2, TNF receptor-associated factor 2; RIP1, receptor-interacting protein kinase 1; FADD, Fas-associated death domain; Bid, BH3 interacting-domain death agonist; IKKα, Inhibitor of kappa B alpha; IKKβ, Inhibitor of kappa B beta; NF-κB, Nuclear factor kappa B; ROS, reactive oxygen species.

During a viral infection, the intrinsic apoptotic pathway can be induced by numerous intracellular responses, all being mediated through the mitochondria. Mitochondrial membrane permeabilization (MMP) is the key step in apoptotic signaling through the mitochondria and is regulated by B-cell lymphoma 2 (BcL-2) family proteins. The BcL-2 family is comprised of three classes of proteins containing Bcl-2 homology regions (BH1-4). BCL-2 associated X protein (Bax) and Bcl-2 homologous antagonist/killer (Bak) function as pro-apoptotic effector proteins that are activated by the pro-apoptotic BH3 only proteins, Bid, Bcl-2-like protein 11 (Bim), p53 upregulated modulator of apoptosis (Puma), Phorbol-12-myristate-13-acetate-induced protein 1 (Noxa) and B lymphocyte kinase (Blk). The anti-apoptotic members of the Bcl-2 family include BcL-2, B-cell lymphoma-extra large (BcL-XL) and Induced myeloid leukemia cell differentiation protein (McL-1). An intracellular death signal induces the activation and oligomerization of Bax or Bak which form pores in the mitochondrial outer membrane (MOM) allowing for the release of pro-apoptotic factors from the inter-mitochondrial space including cytochrome c, apoptotic protease activating factor 1 (Apaf1), and the second mitochondria-derived activator of caspases/ direct inhibitor of apoptosis-binding protein with low pI (SMAC/Diablo) (Kiraz et al. 2015; Upreti et al. 2008). Cytochrome c binds to Apaf1 and recruits caspase 9 to form what is known as the apoptosome (Yuan et al. 2013). Apoptosis occurs by the activation of effector caspases 3, 6 and 7 (Kiraz et al. 2015). SMAC/Diablo antagonizes anti-apoptotic inhibitors of apoptosis (IAP) proteins thus removing the inhibition on the formation of the apoptosome (Green & Llambi 2015; Kiraz et al. 2015). The intrinsic and extrinsic pathways are not

mutually exclusive wherein activation of one pathway typically leads to secondary activation of the other pathway. An alternative activation of the intrinsic pathway is through Bid cleavage by caspase 8 which leads to MMP activated by extrinsic apoptotic signals initiated at the TNF family receptors (Kiraz et al. 2015).

Poxviruses encode numerous viral BcL-2-like proteins (vBcL-2) that function to antagonize and modulate the apoptotic signal induced by host death response mechanisms. VACV contains at least 5 vBcL-2 proteins that all function to modulate various aspects of apoptosis at the mitochondria (Boya et al. 2004). So far, no equivalent proteins have been found in MCV.

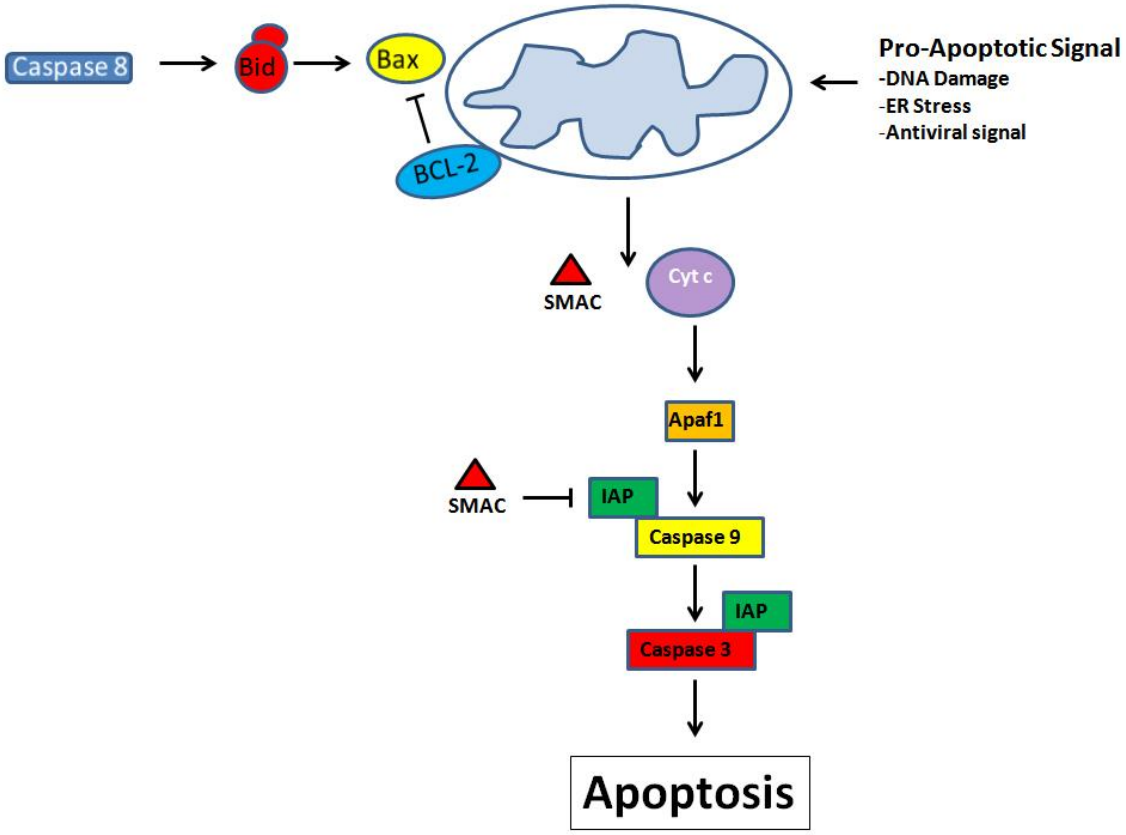

Figure 2: Intrinsic Apoptosis Pathway: Pro-apoptotic stimuli cause the permeabilization of the mitochondrial outer membrane causing the release of pro-apoptotic factors including SMAC and cytochrome c. SMAC binds IAP allowing for the activation of caspase 9 and caspase 3. Cytochrome c binds Apaf1 and recruits caspase 9 to form the apoptosome which activates the effector caspase 3 leading to apoptosis. Bid, BH3 interacting-domain death agonist; Bax, BCL-2 associated X protein; Cyt c, cytochrome c; BcL-2, B-cell lymphoma 2; Apaf1, apoptotic protease activating factor 1; IAP, inhibitor of apoptosis; SMAC, second mitochondria-derived activator of caspases; DNA, deoxyribonucleic acid; ER, endoplasmic reticulum.

Another pathway that is activated in response to a viral infection is the MAVS signaling pathway in which over-expression of the MAVS protein has been shown to induce apoptosis (Lei et al. 2009). MAVS mediated signaling involves the recruitment of Heat-shock protein 90 (HSP90), the IKK complex (Inhibitor of nuclear factor kappa-B kinase (IKK) alpha, -beta and -epsilon (IKKα, $-\beta$, $-\varepsilon$)) and TANK binding kinase 1 (TBK1) which elicit the production of INF's through activation of the interferon regulatory factor 3 (IRF3) and NF-κB transcription factors (Huang et al. 2014; Amaya et al. 2014). Viral modulation at the MAVS complex has been shown with MC159 interactions blocking TBK1 signaling through the direct interaction with TBK1 and MC160 preventing TBK1 activation through a still undetermined mechanism (Randall et al. 2013). If the MAVS complex is disrupted, Bax is imbedded into the mitochondrial membrane causing MMP and subsequent activation of apoptosis (Chattopadhyay et al. 2010). Another signal pathway mediated by MAVS is through the recruitment of FADD and Pro-caspase 8 which mediates apoptosis similar to the activation of apoptosis through extrinsic signals (Maadidi et al. 2014).

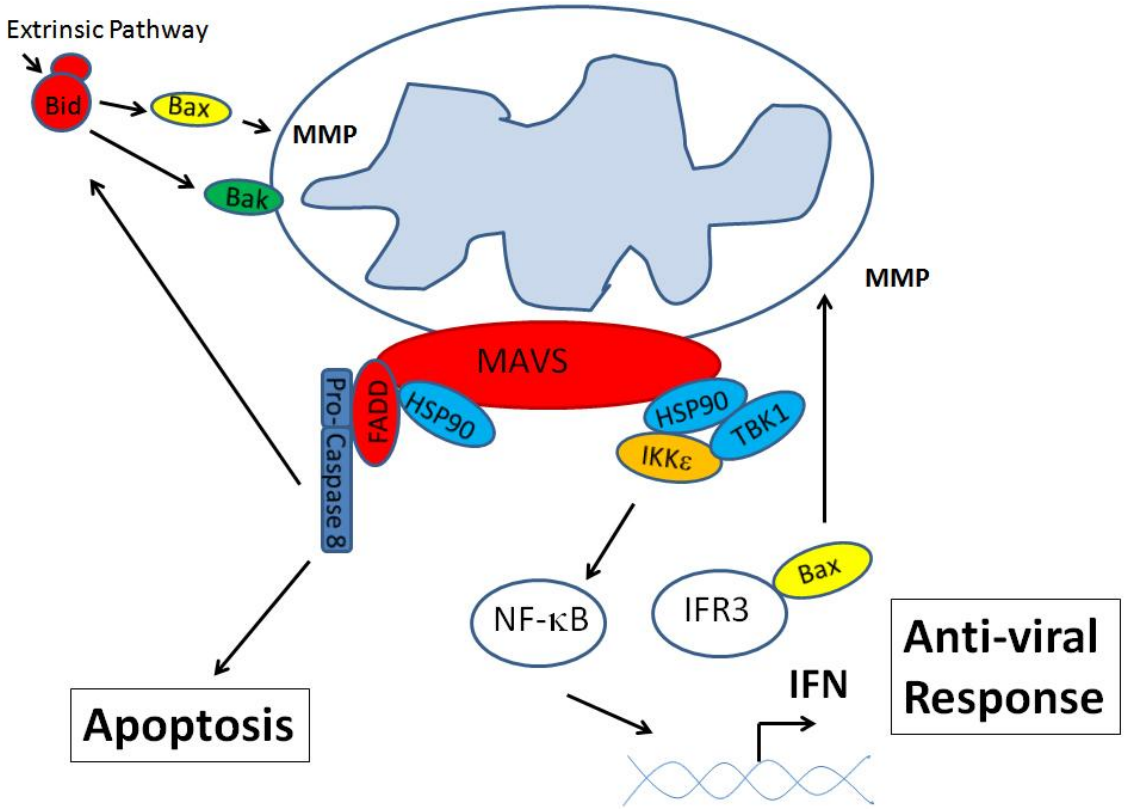

Figure 3: MAVS-induced Apoptosis Pathway. Activation of the MAVS-induced antiviral response occurs downstream of cellular danger sensors. Recruitment of Hsp90, TBK1 and IKKε to the MAVS complex lead to activation of transcription factors (NF-κB, IRF3) and promote cell survival, inflammation and the production of interferon's, whereas, recruitment of the Hsp90, FADD, and procaspase 8 lead to apoptosis. MAVS, mitochondrial antiviral signaling protein; HSP90, Heat-shock protein 90; FADD, Fas-associated death domain; Bid, BH3 interacting-domain death agonist; TBK1, TANK binding kinase 1; IKKe, Inhibitor of nuclear factor kappa-B kinase epsilon; Bax, BCL-2 associated X protein; IRF3, ; NF-kB, Nuclear factor kappa B; IFN, Interferon; MMP, mitochondrial membrane permeabilization.

Lack of a cell culture or animal model to study MCV severely hampers efforts to understand MCV immune evasion strategies. Current efforts to understand MCV pathogenesis are being done studying primary lesions and the use of a luciferase reporter based system, but this approach can lead to experimental difficulties resulting from MCV strain variations and large differences in viral yields between lesions (Sherwani et al. 2012). The approach taken in this report was to isolate a particular gene product of MCV and to study the role on apoptotic processes *in vitro* by transient transfection. The advantages of this system are the relative ease of implementation and the wide range of studies that can be done relatively quickly. The downside is that all of the results need to be taken with the understanding that the results obtained here may or may not represent what would be seen in an actual viral infection. A more detailed review of current strategies for studying MCV can be found in Shisler 2015.

The purpose of this thesis was to characterize a novel MCV protein, MC163, and determine its role in the modulation of apoptosis. Bioinformatics analysis of the MC163R ORF revealed a mitochondrial localization sequence (MLS), a metal binding domain and a putative transmembrane domain. Since all viral proteins that localize to the mitochondria have a role in the modulation of death pathways, the working hypothesis is that MC163 modulates apoptosis. Mutants of MC163R were made by splitting the full length protein at a predicted protease site. A mutant lacking the MLS could give valuable clues as to the function and role of MC163R in apoptosis. The role of MC163 in apoptosis was assessed by JC-1 staining as an indicator of mitochondria membrane permeabilization, a hallmark in both extrinsic and intrinsic apoptosis pathways.

Materials and Methods

Expression vectors for MC163R Mutants:

To construct the C-terminal mutant plasmid, the MCV genomic plasmid library (a gift from Dr. Joachim J. Bugert) containing ORF MC163R was amplified by PCR using the forward primer MC163Pr3For, 5'- TTT TC GAATTC G CCA TGT TGT CGC CGG CGG AC-3', containing the EcoRI restriction site (underlined), and reverse primer, MC163.HARev1, 5'- GTC ATA CGG GTA CAG CGC GCC CTC CG -3', containing the first half of the HA tag. Subsequent PCR was done to add the second half of the HA oligonucleotide sequence using the forward primer MC163Pr3For, and the reverse primer, MC163.HARev2, 5'- AAT TCTAGA TTA GGC ATA GTC CGG CAC GTC ATA CGG GTA C -3', containing the XbaI restriction site (underlined). The amplified sequence was digested using EcoRI/XbaI cloned into the pCI vector (Promega). Multiple attempts were made to clone the N-terminal and full length MC163 constructs. However, the high GC rich content in the upstream region of MC163R made cloning the N-terminal portion difficult. To circumvent this problem, the N-terminal region of MC163R (MC163N, a.a. 1-132) was codon optimized and synthesized *in vitro* by GenScript and inserted into pcDNA3.1-HA. To construct the full length MC163R plasmid, overlapping PCR was used by amplifying the N-terminal portion from the synthesized MC163N construct by PCR using the forward primer MC163NGSFor, 5'- TCC GAA TTC GCC ACC ATG GGA CCA AGA G-3', and reverse primer, MC163NGS Rev, 5'- GGC TCG CTA TGG TTC CAG AAG ACC TGC CTC TCC AG-3'. The C-terminal portion was amplified from the MC163C/pCI construct made previously by PCR using the forward

primer, MC163C_For, 5'- GAG AGG CAG GTC TTC TGG AAC CAT AGC GAG CCT C-3', and the reverse primer, MC163.CRevHA2. The N-terminal and C-terminal sequences were PCR amplified using MC163NGSFor and the reverse primer MC163 to generate the full length MC163 construct,.CRevHA2. All constructs were engineered to contain a C-terminal HA-tag. Constructs were cloned into the pCDNA3.1 vector and sequenced (Genewiz) to verify the correct nucleotides. PCR conditions used can be found in Table 3.

Plasmid DNA preparations:

Plasmid DNA was isolated from bacterial cultures using the PureYield Plasmid Miniprep system (Promega) according to the manufactures protocol. Briefly, bacteria (DH5α, TOP10, BL-21) harboring plasmid inserts containing experimental constructs were grown for 16-20 hours in Luria broth supplemented with the proper antibiotic (ampicillin, 100 μg/mL, Life Technologies; kanamycin, 50 μg/mL). Bacteria were harvested by centrifugation at 14,000 rpm for 1 minute, resuspended in 600mL of Tris-EDTA buffer (TE) and the Promega protocol was followed. Plasmid DNA was eluted in TE buffer, assessed for purity and concentration using a Nanovue Plus spectrophotometer and stored at 4^{o}C. OD_{260}/OD_{280} values of 1.8-2.0 were deemed acceptable and utilized in subsequent experiments.

Cell culture and Transfections

Human embryonic kidney 293T (HEK 293T) and HeLa cells were maintained in Dulbecco's modified eagle medium (DMEM, Sigma or HiMedia) supplemented with

10% fetal bovine serum and 1% penicillin-streptomycin (Sigma) at 37^{o}C, with 5% CO_2 in a humidified incubator. Stable transfected HeLa cell lines (HeLa-163F, HeLa-163C, HeLa-163N) were maintained as described above with the addition of the selection marker, G-418 (Life Technologies, 1mg/mL) to the growth media. Transfection of HEK293T cells or HeLa cells was performed using Mirus Trans-IT 2020 reagent in Opti-MEM (Gibco/Life Technologies) at 3 μL/μg or 2 μL/μg of total DNA, respectively.

Immunoblotting

HEK293T cells or HeLa cells were harvested using RIPA lysis buffer supplemented with protease inhibitor cocktail added according to the manufactures recommended concentration (Amresco, M250: AEBSF, Aprotinin, E-64, Bestatin, Leupeptin, Pepstatin) and assayed for total protein content using the BCA assay (Pierce) for total protein according to the manufactures protocol (Thermo Scientific). Samples were boiled for 5 minutes with 5% 2-mercaptoethanol in sodium dodecyl sulfate (SDS) sample buffer (62.5 mM Tris pH 6.8, 2% SDS, 10% Glycerol, 100 mM DTT, 0.01% bromophenol blue) and placed on ice until use. Lysates were resolved by 10% SDS-PAGE, transferred to polyvinylidene difluoride (PVFD) membranes (Millipore), blocked in 5% milk (Carnation non-fat dry milk) in 1X Phosphate-buffered saline with Tween® 20 (PBST, 50 mM Tris.HCl, pH 7.4, 150 mM NaCl, 0.1% Tween 20) for 30 minutes and probed for 1 hour using the appropriate antibody (α-HA, 1:2,500; α-PARP-1, 1:1,250; α-FLAG, 1:2,500) diluted in 0.5% milk in TBST. The PVDF membranes were washed three times with 0.5% milk in TBST then incubated with secondary antibodies (goat-α-

mouse-HRP, 1:10,000; goat-α-rabbit-HRP, 1:10,000; HRP, horseradish peroxidase) for 1 hour, washed three times with 0.5% milk in TBST then visualized using SuperSignal™ West Pico or SuperSignal™ West Femto (Thermo Scientific) chemiluminescent reagent according to manufactures instruction. Blots were visualized using a FluorChem E imaging system (Protein Simple).

JC-1 Staining for Detection of Mitochondrial Membrane Permeabilization

Subconfluent HeLa cells were transfected with either pCDNA3.1 (500 ng); pHA-MC159 (500 ng), pHA-MC163F (500 ng), pHA-MC163N or pHA-MC163C (500 ng). Twenty four hours later cells were treated with TNF-α (10 ng/mL) and cyclohexamide (CHX, 10 ng/mL) or CCCP (Carbonyl cyanide m-chlorophenyl hydrazone, 100μM) and incubated at 37°C for 6 hours (TNF-α) or 30 minutes (CCCP) in a 5% CO_2 humidified incubator. Cells were stained with JC-1 (5,5′,6,6′-tetrachloro-1,1′,3,3′-tetraethylbenzimi-dazolylcarbocyanine iodide, Cayman Chemical, 1 μM) and incubated in a 5% CO_2 incubator at 37°C for 20 minutes in the dark. Immediately after incubation, the cells were analyzed by confocal microscopy (Olympus, Monomer detection: Ex/Em = 514 nm/529 nm, J-aggregate detection: Ex/Em = 585 nm/590 nm). Multiple images were taken for each condition using constant voltage settings and analyzed with ImageJ software using the Fiji image processing package (Schindelin, et al. 2012). Composite images were split into separate color channels, binarized and analyzed for % area for each color. The ratio of J-aggregate to monomer form of JC-1 was calculated and normalized to the control.

This experiment was repeated 5 times (n=5) with a minimum of 3 images taken for each condition in each experiment.

Lucerifase Assay

HEK293T cells were plated at 2.5 x 10^5 cells per well in a 12-well plate and grown for 24 hours at 37^{o}C in a 5% CO_2 humidified incubator. After 24 hours, the cells were transfected with 500 ng of plasmid DNA (pCDNA3.1, pHA-MC159, pHA-MC163F, pHA-MC163C or pHA-MC163N), 225 ng reporter plasmids (200 ng pNF-kB-Luciferase or pIFN-b-luciferase, 25 ng pRenilla TK) and 275 ng of pCDNA3.1 using Mirus Trans-IT 2020 reagent (Mirus) at a ratio of 3 μL/μg of total DNA. The cells were then incubated for another 24 hours at 37^{o}C in a 5% CO2 incubator prior to treatment with 10 ng/mL TNF-α. 6-8 hours? post treatment, the cells were lysed at room temperature for 30 minutes with 1X passive lysis buffer (Promega) supplemented with protease inhibitors added according to manufactures recommended concentration (Amresco, M250: AEBSF, Aprotinin, E-64, Bestatin, Leupeptin, Pepstatin). The lysates were assayed for firefly and sea pansy luciferase activity using the Dual-reporter assay according to manufactures instructions (Promega). Statistical significance was determined by utilizing the student's t-test.

Immunofluorescence and confocal microscopy for localization of MC163R mutants:

HEK293T cells or HeLa cells were plated at 2.5 x 10^5 cells per well on glass coverslips in a 12-well plate and grown for 24 hours at 37^{o}C in a 5% CO_2 humidified incubator. After 24 hours, the cells were transfected with 1 μg of plasmid DNA

(pCDNA3.1, pHA-MC163F, pHA-MC163C or pHA-MC163N) and 500 ng pmTurquoise2-Mito [pmTurquoise2-Mito was a gift from Dorus Gadella (Addgene plasmid # 36208))] using Mirus Trans-IT 2020 reagent (Mirus) at a ratio of 3 μL/μg (HEK293T) or 2 μL/μg (HeLa) of total DNA. The cells were then incubated for another 24 hours at 37^{o}C in a 5% CO_2 incubator prior to fixation with 4% paraformalyhyde (Mpbio) for 1 hour at 4^{o}C. Cells were rinsed twice with PBS, permeabilized with 0.5% Triton X-100 for 5 minutes, rinsed with PBS twice, incubated with 50 mM glycine for 10 minutes then blocked with 5% milk (Carnation non-fat dry milk) in 1X Phosphate-buffered saline with Tween® 20 (PBST, 50 mM Tris HCl, pH 7.4, 150 mM NaCl, 0.1% Tween 20) for 30 minutes. To detect MC163R mutants, the cells were incubated with an anti-HA (Sigma Aldrich) conjugated to an Alexa Fluor^{TM} 647 dye (Thermo Fisher antibody labeling kit) for 1 hour at 18-22^{o}C, rinsed three times with 0.5% milk in PBST for 10 minutes, rinsed twice with PBST for 15 minutes then mounted to microscope slides with 50% glycerol in PBS. The plasmid pmTurquoise2-Mito encodes a cyan-fluorescent protein that localizes to the mitochondria (Stetten, et al. 2012). Fluorescence was detected using an Olympus microscope (software) for pmTurquoise2-Mito (Ex = 488 nm, Em = 519 nm) and MC163R mutants (Ex = 633 nm, Em = 671 nm). Images were false colored using Olympus Fluoview software and exported as JPEG files for each of the fluorescence signals.

Results

Cloning the MCV MC163 Gene:

The goal of our research was to identify novel MCV immune evasion molecules. MC163R was previously reported to contain a putative Cu^{2+}/Zn^{2+} binding domain (REF; amino acids (a.a.) 46-108, Figure 4). Our bioinformatics analysis revealed the presence of a mitochondrial localization sequence (MLS) located in the N-terminus portion of MC163R (a.a. 1-30, (http://psort.ims.u-tokyo.ac.jp/) and a putative transmembrane domain (TMD, a.a. 109-132,) immediately downstream of the predicted metal binding domain (a.a. 30-46) (http://www.ch.embnet.org/software/TMPRED_form.html). The predicted TMD is flanked by positively charged amino acids similar to other mitochondrial outer membrane (MOM) proteins anchored by the N-terminus, for example, Tom70 (translocase of the outer mitochondrial membrane 70) (Rapoport, D., 2003; Figure 6). Further analysis of the C-terminal portion of MC163R identified no regions of homology in the amino acid sequence to other viral or host proteins. MC163R protein folding representations using Phyre2 server and iTasser prediction website, respectively, can be seen in Figure 7. MC163R contains a GC rich upstream region which made cloning of this gene particularly difficult. To circumvent this problem the N-Terminal portion of MC163R (MC163N, a.a. 1-132) was synthesized *in vitro*, while the C-terminal region (MC163C, a.a. 132-620) was cloned using PCR (Figure 5, Table1, Table 2). The synthesized MC163N construct was codon optimized (Figure 8) to remove high GC content, but maintained the wild-type amino acid sequence (Figure 9). Overlapping PCR was used to generate the full length construct (MC163F, a.a. 1-620)

(Figure 5, Table 1, Table 2). All constructs were engineered to contain a C-terminal HA epitope tag to detect expression. PCR amplicons were cloned into the pCDNA3.1 vector and sequenced. Expression of the constructs in HEK293T cells was verified by immunoblotting and detection with anti-HA antibodies (Figure 10A). Both the MC163F and MC163C were easily detected at 67 kD and 50 kD respectively. We also detected a 50 kD product in the MC163F lanes corresponding to a predicted cleavage site in between the N- and C-terminal MC163 constructs. Relative to MC163F and MC163C, MC163N expressed at lower levels, but was detected as a band of approximately 17 kD with longer exposure time (Figure 10B).

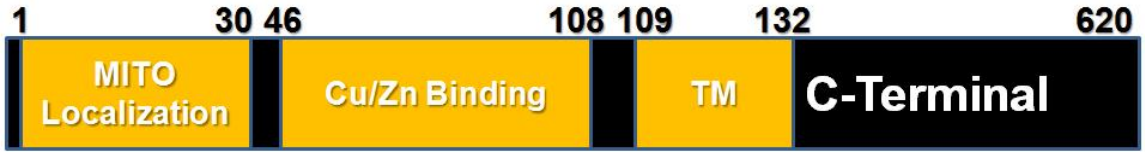

Figure 4: Representation of domains predicted by bioinformatics in MC163R.

Mitochondrial localization sequence was identified using ipSORT prediction website (Bannai et al. 2001; Bannai et al. 2002) and TargetP 1.1 Server (Emanuelsson et al. 2000)

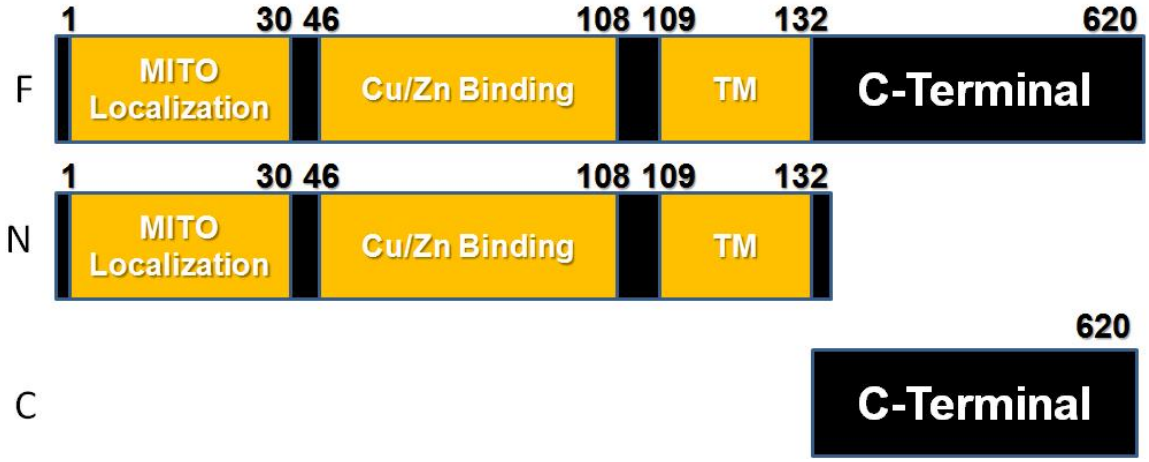

Figure 5: MC163R mutants characterized in this study. Full length, a.a. 1-620; N-terminal mutant, a.a. 1-132; C-terminal mutant, a.a. 132-620

A)

MC163R (MCV) **RH**G**R**AP**RR** LALTAPLPLLLLPLLLPPMILLFF LSPADA**K**PVLE**R**
TOM 70 (H.s.) P**R**WQ LALAVGAPLLLGAGAIYLWS **R**QQ**RRR**EA**R**G**R**

B)

Metal Binding Domain

MC163R (MCV) E**H**GYA**HTH**TCEDTPAKE**H**G**H**LGE**H**ECLRG**H**G**H**A**H**AYEERCENK**H**K**H**L**H**A**H**E**H**T**H**ER**H**GRAPRR

C)

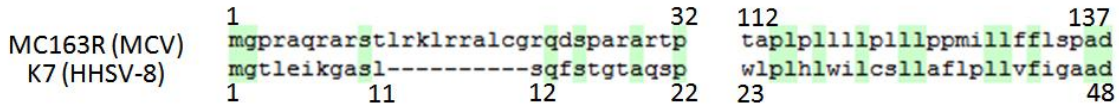

Figure 6: Amino acid sequence of the predicted transmembrane domain and Metal Binding domain of MC163R. A) The N-terminal portion of MC163R contains a hydrophobic sequence flanked by positively charged amino acids similar to TOMM70, a mitochondrial outer membrane (MOM) resident protein. Hydrophobic sequence is underlined, Bold indicate positive charged amino acids. MCV, *Molluscum Contagiosum* virus, H.s., *Homo sapiens*. B) Histidine rich metal binding domain of MC163R (a.a. 46-108). C) Amino acid alignment of MC163R and HHSV-8 K7 protein.

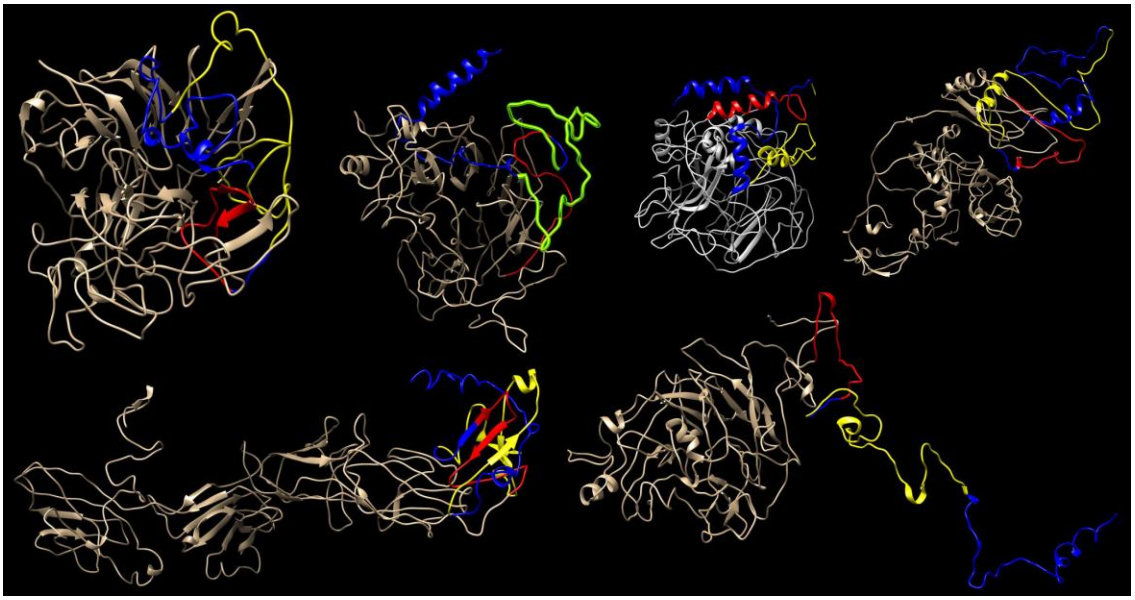

Figure 7: MC163F protein folding predictions using Phyre2 (A) and iTasser (B-F) predictions. Blue, Mitochondrial localization sequence; Yellow, Metal binding domain; Red, Transmembrane domain; Grey, C-terminal domain.

Primer Name:	Primer Sequence:
MC163Pr3For	5'- TTT TCG AAT TCG CCA TGT TGT CGC CGG CGG AC-3'
MC163C_For	5'- GAG AGG CAG GTC TTC TGG AAC CAT AGC GAG CCT C-3'
MC163NGSFor	5'- TCC GAA TTC GCC ACC ATG GGA CCA AGA G-3'
MC163.HARev1	5'- GTC ATA CGG GTA CAG CGC GCC CTC CG -3'
MC163.HARev2	5'- AAT TCT AGA TTA GGC ATA GTC CGG CAC GTC ATA CGG GTA C -3'
MC163NGS Rev	5'- GGC TCG CTA TGG TTC CAG AAG ACC TGC CTC TCC AG-3'

Table 1: Polymerase chain reaction primer sequences used for cloning MC163R Mutants. Primers MC163Pr3For, MC163.HARev1 and MC163.HARev2 were used to clone the C-terminal mutant into the pCI vector. Primers MC163NGSFor and MC163NGSRev were used to produce the N-terminal portion of the full length clone with MC163C_For and MC163.HARev2 to produce the C-terminal portion. Overlapping PCR was used to create the full length clone using the MC163NGSFor forward primer and the MC163.HARev2 reverse primer.

Mutant	Vector backbone	Forward Primer	Reverse Primer
MC163C	pCI	MC163Pr3For	MC163.HARev1, MC163.HARev2
MC163C	pCDNA3.1	MC163C_For	MC163.HARev2
MC163N	pCDNA3.1	MC163NGSFor	MC163NGS Rev
MC163F	pCDNA3.1	MC163NGSFor	MC163.HARev2

Table 2: Polymerase chain reaction primers used to construct MC163 Mutants.

```
Optimized    13   ATGGGACCAAGAGCCCAGAGAGCAAGATCAACACTGAGAAAACTGAGGAGAGCACTGTGC
Original     13   ATGGGCCCGCGCGCGCAGCGCGCGCGTAGTACGCTACGCAAGCTGAGGCGTGCGTTATGC

Optimized    73   GGAAGGCAGGACAGCCCAGCCAGAGCCCGAACTCCCGAGAACCGACATTTCGCTCGGAAG
Original     73   GGGCGTCAAGACTCGCCCGCGCGCGCGCGAACGCCAGAAAACAGGCACTTCGCACGCAAA

Optimized   133   TGCGCAAGAACCTGTGAACACGGGTACGCCCACACCCATACATGCGAGGACACCCCTGCT
Original    133   TGCGCGCGAACGTGCGAACACGGATACGCGCACACCCACACGTGCGAGGATACGCCCGCG

Optimized   193   AAAGAACACGGACATCTGGGAGAGCACGAATGCCTGAGGGGACACGGACATGCACACGCT
Original    193   AAAGAACACGGACACTTGGGAGAACACGAGTGCTTGCGCGGCCATGGTCACGCGCACGCG

Optimized   253   TATGAGGAACGCTGTGAGAATAAGCATAAACACCTGCATGCCCACGAGCATACACACGAA
Original    253   TACGAAGAGCGATGCGAGAACAAGCACAAACACTTACATGCGCACGAGCACACGCACGAG

Optimized   313   AGGCACGGACGAGCACCTCGGAGACTGGCACTGACTGCACCACTGCCACTGCTGCTGCTG
Original    313   CGCCACGGCCGCGCACCGCGAAGATTGGCGTTGACGGCACCGCTACCGTTGCTATTGCTG

Optimized   373   CCACTGCTGCTGCCCCCTATGATTCTGCTGTTCTTTCTGAGCCCCGCTGACGCAAAACCC
Original    373   CCACTGCTATTACCGCCGATGATACTTTTGTTCTTCTTGTCGCCGGCGGACGCAAAGCCC

Optimized   433   GTGCTGGAGAGGCAGGTCTTC
Original    433   GTGCTCGAGAGACAAGTCTTC
```

Figure 8: DNA sequence comparison of wild type MC163N vs GenScript codon optimized MC163N.

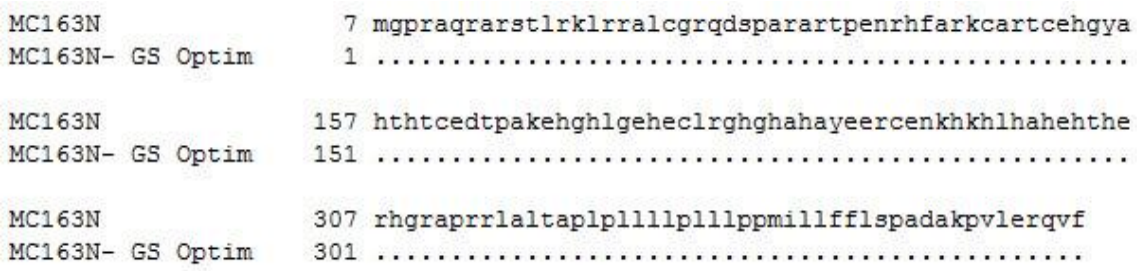

Figure 9: The protein alignment for wild-type MC163N and codon optimized MC163N (GenScript). Amino acid sequence comparison shows the codon optimized DNA sequence maintains the wild-type amino acid sequence.

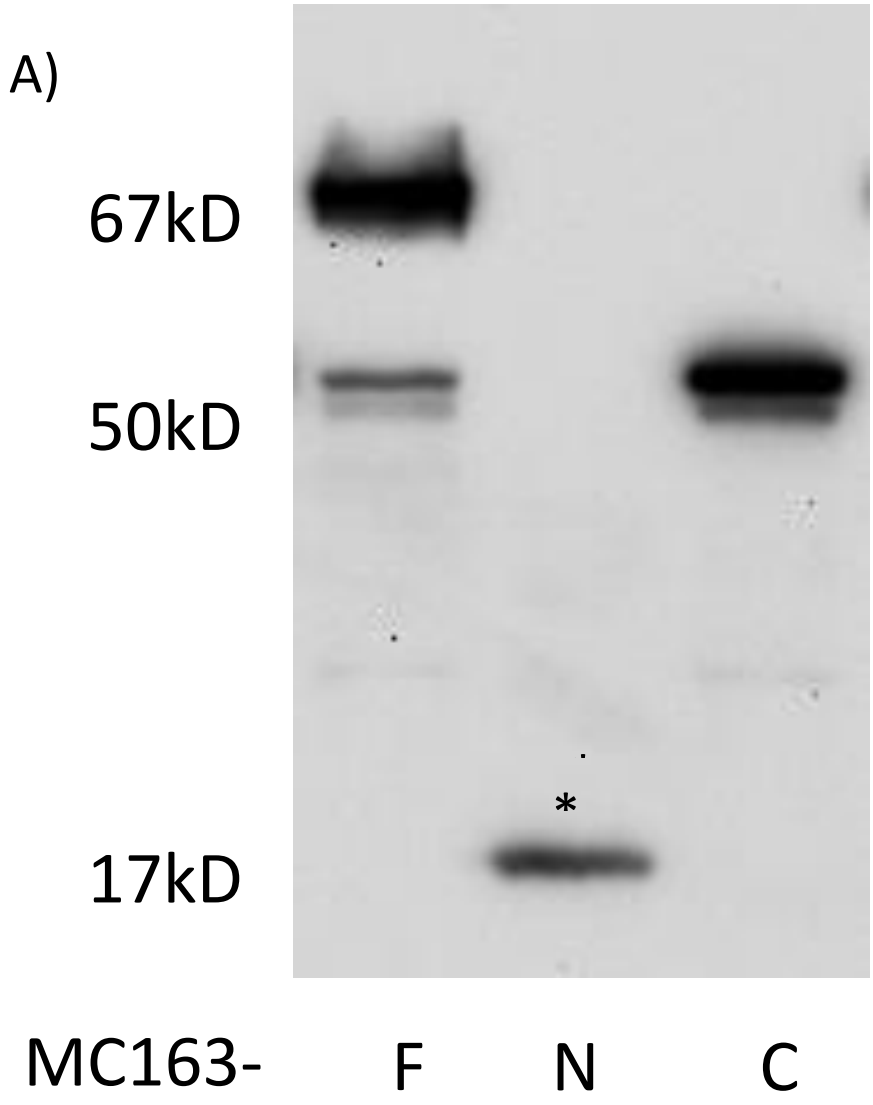

Figure 10: The expression of MC163R mutants by immunoblotting. A) MC163F and MC163C were readily detected. MC163N, however, expressed at weaker levels then MC163F and MC163C and additional detection time was required to observe MC163N (*).

The N-terminal portion of MC163 is required for mitochondrial localization

To determine the localization of the MC163R constructs, HeLa cells were co-transfected with the indicated MC163R construct and pmTurquise2Mito, a cyan fluorescent protein engineered to contain a mitochondrial localization sequence (Goedhart, J., et al, 2012). For detection of MC163R constructs, HeLa cells were incubated with an anti-HA antibody conjugated to an Alexa Fluor 647 dye to ensure that no overlap was seen between the two detection channels. The excitation and emission spectra for pmTurquise2Mito is Ex/Em = 488 nm/519 nm and the anti- HA antibody conjugated to Alexa Fluor™ 647 dye is Ex/Em = 633 nm/671 nm. Both MC163F and MC163N contain the mitochondrial localization sequence and were readily detected to co-localize with the mitochondrial marker pmTurquise2Mito (Figure 11, Top and Bottom panels). MC163C, however, which lacks both the MLS and the putative transmembrane domain, did not localize to the mitochondria, but was detected in a diffuse staining pattern throughout the cell (Figure 11, Middle panel). It is worth noting that the deletion of the entire C-terminal region of MC163 did not affect the localization of the N-terminal (MC163N) mutant. Therefore, we conclude the N-terminal portion of MC163R is required for mitochondrial localization.

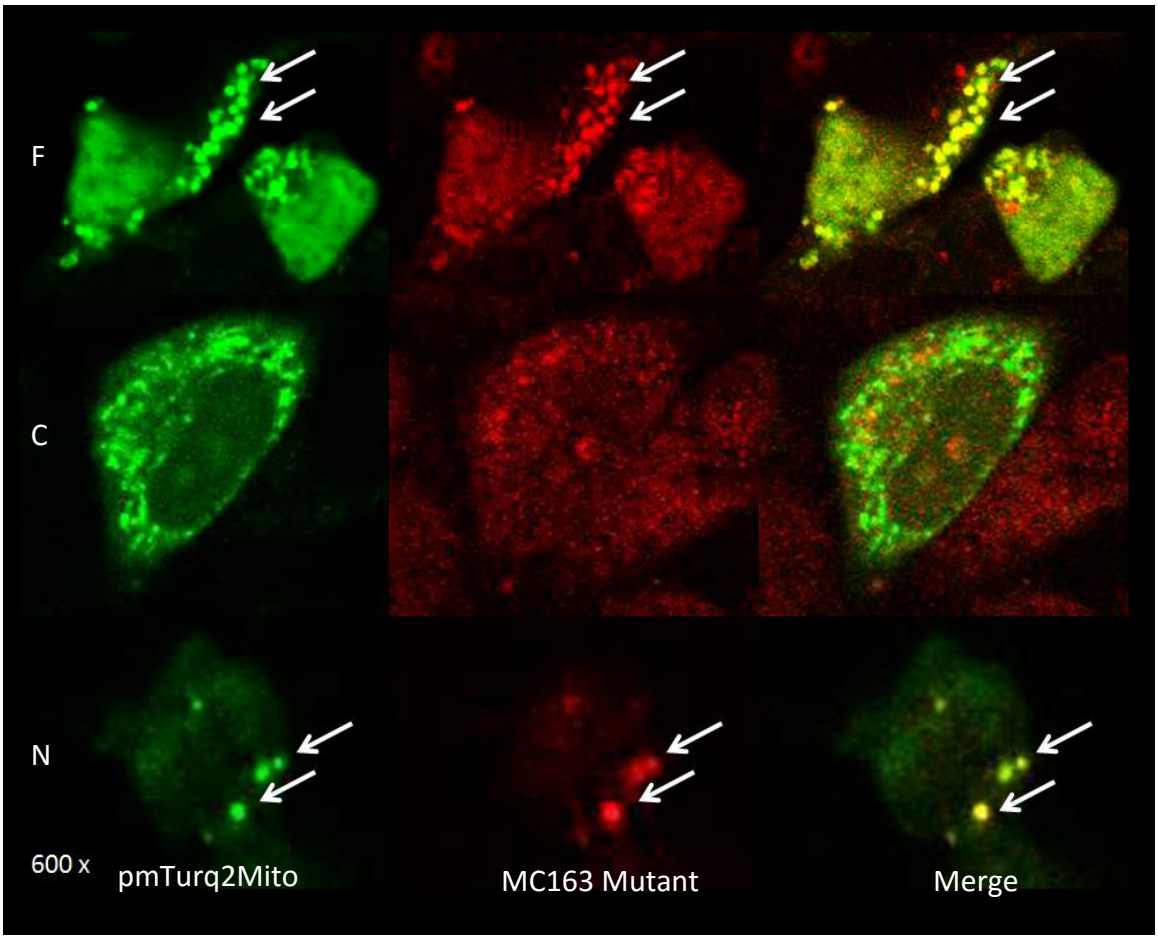

Figure 11: Localization of MC163R mutants. Mitochondrial localization was confirmed for MC163F and MC163N mutant (Top and Bottom panels). MC163C mutant does not localize to the mitochondria (Middle panels). Colocalization was done with a mitochondria localizing fluorescent protein, pmTurquise2Mito (green). MC163R mutants were labeled using an α-HA antibody conjugated with an Alexa Flour 647 (α-HA:AF647) dye. Images were acquired using an Olympus confocal microscope (pmTurquise2Mito: Ex/Em = 488 nm/519 nm; α-HA:AF647: Ex/Em = 633 nm/671 nm) and processed using Olympus FluoView Ver4.2 software. Co-localization events are depicted with white arrows. F, MC163F; C, MC163C; N, MC163N.

MC163R inhibits TNF-α-induced mitochondrial membrane permeabilization

As of the date of this report, all viral proteins that localize to the mitochondria have been shown to modulate cellular death pathways. Therefore, the working hypothesis was that MC163R dampens the extrinsic apoptotic pathway. To examine the effect of MC163R on mitochondrial membrane permeabilization (MMP) we utilized the cationic dye JC-1. JC-1 forms J-aggregates in the mitochondria that fluoresce with an emission maximum at 590 nm and also forms monomers when diffuse in the cytoplasm with an emission maximum at 529 nm. Treatment with TNF-α induces MMP and can be seen as a shift from J-aggregate to monomer JC-1 which can be detected by confocal microscopy. Treatment with TNF-α (10ng/mL) and cycloheximide (CHX, 10ng/mL) induced MMP in cells transfected with empty vector and was detected by the loss of the J-aggregate JC-1 signal (Figure 12). In contrast, cells expressing pHA-MC159, an MCV protein that antagonizes both Fas and TNF-induced apoptosis by binding FADD and procaspase-8 (Thome et al. 1997; Shisler & Moss 2001; Nichols & Shisler 2009), were protected from MMP (Figure 12). Cells expressing MC163F and MC163N were protected from TNF-α-induced MMP similar to MC159. In contrast, cells expressing MC163C, which lack the ability to localize to the mitochondria, resulted in the loss of the mitochondria membrane potential and subsequent MMP similar to cells expressing empty vector alone (Figure 12). The results were quantified using ImageJ software using the Fiji image processing package (Schindelin, J., et al., 2012). The ratio of J-aggregate to monomer form of JC-1 was calculated and normalized to the control. TNF-α treatment of cells expressing vector alone resulted in a shift from J-aggregate to monomer JC-1

indicating a loss of mitochondrial membrane potential and MMP. In contrast, the J-aggregate to monomer ratio of MC159, MC163F and MC163N expressing cells remained unchanged after TNF-α/CHX treatment, whereas MC163C expressing cells resulted in a shift in the J-aggregate to monomer ratio similar to vector alone (Figure 13). Taken together, our data indicates that the N-terminal region of the MC163R protein is required to prevent MMP induced by TNF-α.

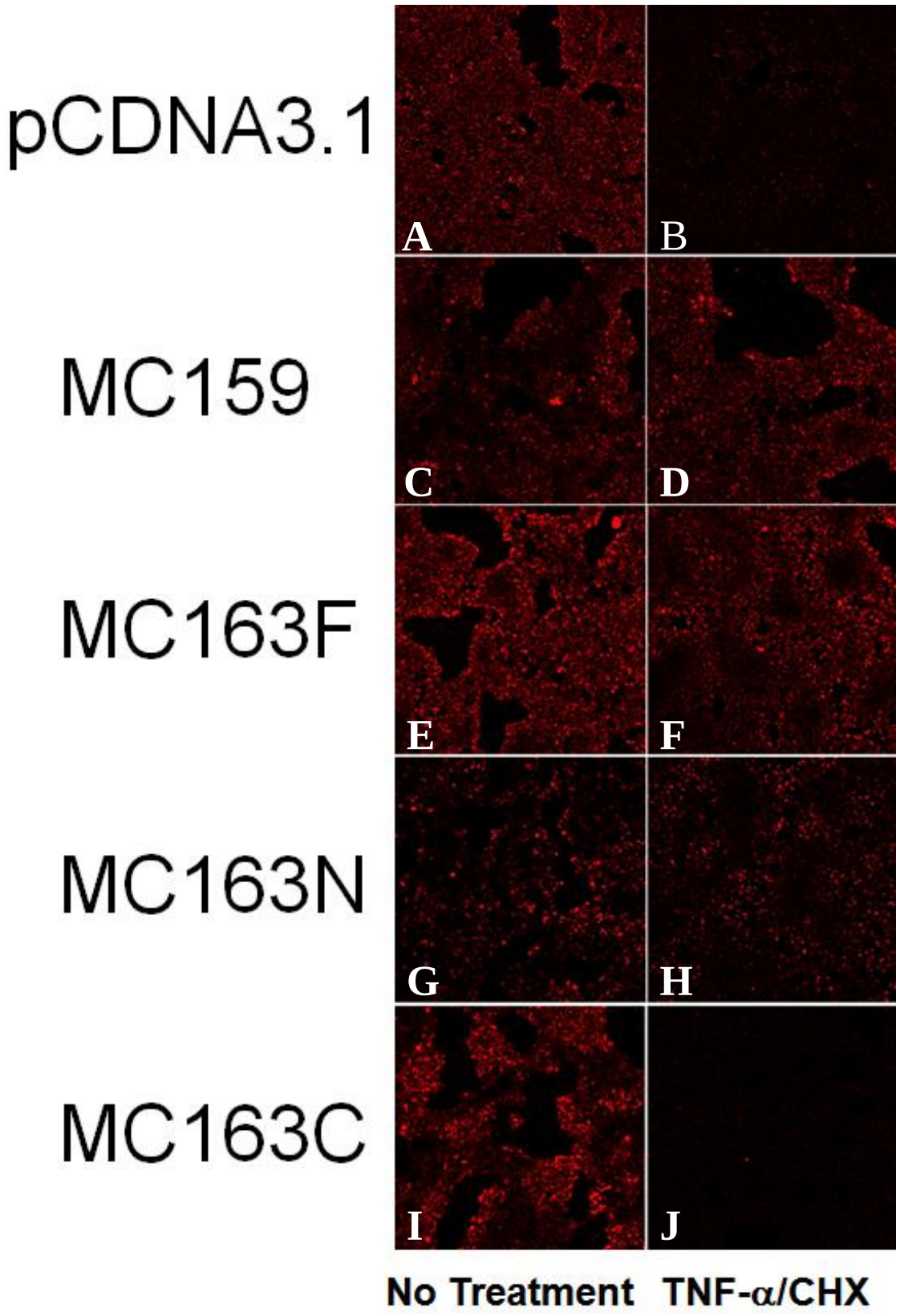
pCDNA3.1
MC159
MC163F
MC163N
MC163C
A
B
C
D
E
F
G
H
I
J
No Treatment
TNF-α/CHX

Figure 12: TNF-α-induced MMP: Mitochondrial membrane permeabilization (MMP) detected by JC-1 staining of HeLa cells with and without TNF-α treatment (10ng/mL, 6 hours). J-aggregate channel is shown (detection: Ex/Em = 585 nm/590 nm). Subconfluent HeLa cells were transfected with pCDNA3.1 (500 ng); pHA-MC159 (500 ng); pHA-MC163F (500 ng); pHA-MC163N; or pHA-MC63C (500 ng) then stained with cyanine dye JC-1 (5,5′,6,6′-tetrachloro-1,1′,3,3′-tetraethylbenzimi- dazolylcarbocyanine iodide, Cayman Chemical) for 20 minutes then immediately imaged using an Olympus confocal microscope. J-aggregate channel is shown (detection: Ex/Em = 585 nm/590 nm). Untreated HeLa cells transfected with pCDNA3.1 (A); pHA-MC159 (C); pHA-MC163F (E); pHA-MC163N (G) and pHA-MC163C (I). MMP in pCDNA3.1 transfected cells (B). No MMP in positive control (pHA-MC159, D). MC163F and MC163N block MMP induced by TNF-α treatment (F, H) MC163C does not block MMP (J). Images represent the J-aggregate form of JC-1 and are shown from one representative experiment, (n=5).

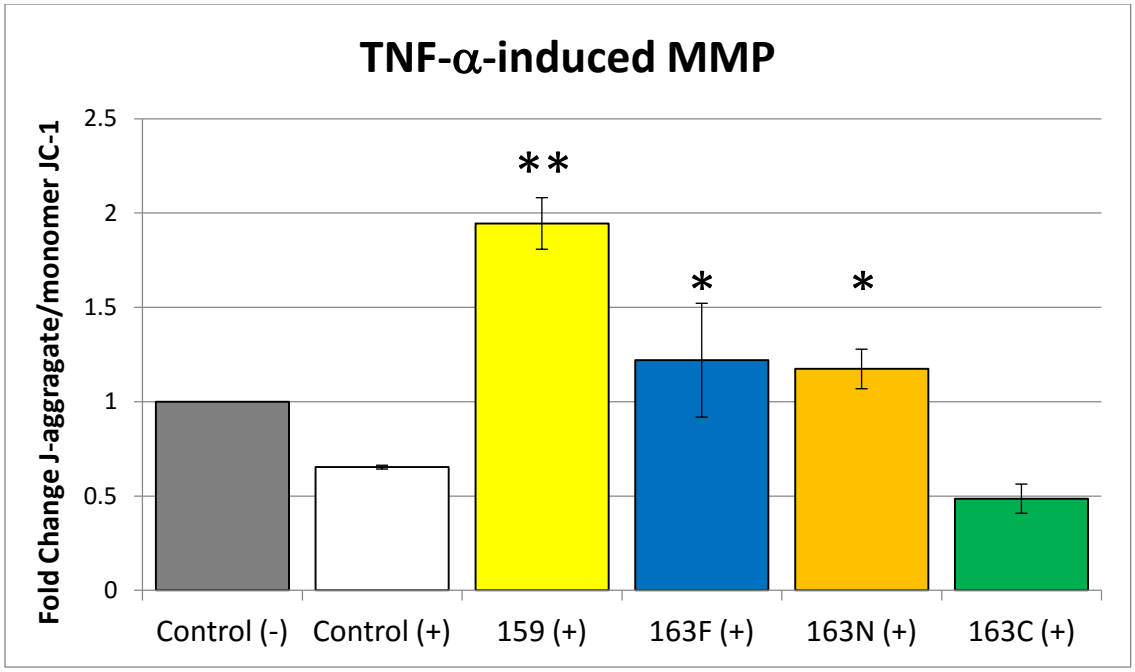

Figure 13: The effect of MC163F on the mitochondrial membrane permeabilization induced by TNF-α treatment. Subconfluent HeLa cells were transfected with pCDNA3.1 (500 ng); pHA-MC159 (500 ng), pHA-MC163F (500 ng), pHA-MC163N or pHA-MC163C (500 ng). Twenty four hours later cells were treated with TNF-α (10 ng/mL) and cyclohexamide (CHX, 10 ng/mL) and incubated at 37^{o}C for 6 hours in a 5% CO_2 humidified incubator. Cells were stained with the cyanine dye JC-1 (5,5′,6,6′-tetrachloro-1,1′,3,3′-tetraethylbenzimi- dazolylcarbocyanine iodide, Cayman Chemical) for 20 minutes then immediately imaged using an Olympus confocal microscope (Olympus, Monomer detection: Ex/Em = 514 nm/529 nm, J-aggregate detection: Ex/Em = 585 nm/590 nm). Multiple images were taken for each sample (minimum = 3 images / sample) and analyzed with ImageJ software using the Fiji image processing package (Schindelin, J., et al. 2012). Values represent the ratio of J-aggregate to monomer form of JC-1 normalized to the control and are shown from one representative experiment, (n=5)

as mean +/- standard deviations (SD). Significant differences between MC163F, MC163N, MC159 and vector control were determined by two-tailed t-test with significance (*) = $P < 0.01$, (**) = $P < 0.001$.

MC163R modulates NF-κB activation induced by TNF-α

In addition to TNF-induced apoptosis, treatment with TNF-a can induce activation of NF-κB. NF-κB is activated by numerous factors including viral infection and modulates the inflammatory response through the transcription of pro-inflammatory cytokines (TNF-α, IL-1, IL-6, IL-12) and immune regulatory molecules (MHC I, TCRα, β) (Oeckinghaus & Ghosh 2009). Viral regulation of NF-κB is a key component to immune evasion. MCV encodes three proteins, MC132, MC159 and MC160, which have been shown to block the activation of NF-κB through different mechanisms targeting the same pathway (Brady et al. 2015; Murao & Shisler 2005; Randall et al. 2012; Struzik et al. 2014; Nichols & Shisler 2006; Nichols & Shisler 2009). Seeing that another poxvirus, Vaccinia virus (VACV) encodes multiple proteins that modulate NF-κB, it is reasonable to assume that MCV might also encode additional proteins to block NF-κB activation (Bahar et al., 2011; Smith et al., 2013). Therefore, we tested if MC163R expression might also affect TNF-α-induced NF-κB activation. HEK293T cells were transfected with either empty vector, pHA-MC160, pHA-MC159, or pHA-MC163F as well as pNK-κB firefly luciferase and pRL-null *Renilla* luciferase. In cells transfected with empty vector, treatment with TNF-α resulted in a significant increase in the levels of NF-κB activation as detected by an increase in firefly luciferase values. Expression of both HA-MC160 and HA-MC159 dampened TNF-induced NF-κB regulated luciferase activity consistent with previous results (Murao & Shisler 2005; Nichols & Shisler 2009). Interestingly HA-

MC163F expressing cells resulted in a two-fold decrease in the relative activation of NF-κB relative to cells transfected with empty vector after TNF-α treatment (Figure 14).

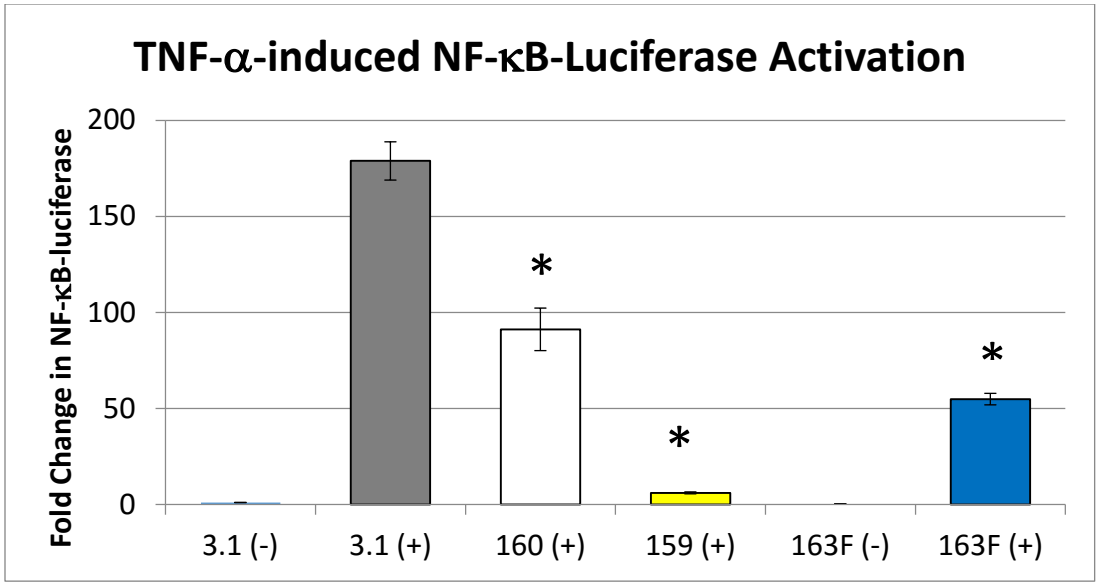

Figure 14: The effect of MC163F on the activation of NF-κB induced by TNF-α treatment. Subconfluent HEK293T cells were transfected with reporter plasmids (pNF-κB-lucerferase, (225ng); pRL-null *Renilla*, (25ng)); pCDNA3.1 (500ng); pHA-MC160 (500ng), pHA-MC159 (500ng) and pHA-MC163F (500ng). Twenty four hours later cells were treated with TNF-α (10ng/mL, 6 hours), lysed in passive lysis buffer supplemented with protease inhibitors and assayed for firefly and sea pansy luciferase activity. Values represent the fold change as compared to untreated empty vector transfected cells (3.1 (-)) and are shown from one representative experiment, run in triplicate (n=3) as mean +/- standard deviations (SD). Significant differences between MC163F, MC160, MC159 and cells transfected with empty vector were determined by two-tailed t-test with significance (*) = $P < 0.001$.

MC163R inhibits CCCP-induced Mitchondrial Membrane Permeabilization

Viruses can induce cellular stress and induce apoptosis in a variety of ways. The mitochondria are a vital component of apoptotic signaling. Given that MC163R localizes to the mitochondria and inhibits TNF-α-induced mitochondrial membrane permeabilization (MMP), MC163 might also protect cells from CCCP-induced apoptosis as well. CCCP (carbonyl cyanide m-chlorophenyl hydrazone) is a protonophore that induces mitochondrial stress by disrupting the proton motive force. Treatment with CCCP (100ng/mL) induced MMP in cells transfected with empty vector and was detected by the loss of the J-aggregate JC-1 signal (Figure 15). In contrast, cells expressing pHA-MC163F were protected from MMP (Figure 15). The results were quantified using ImageJ software using the Fiji image processing package (Schindelin et al. 2012). The ratio of J-aggregate to monomer form of JC-1 was calculated and normalized to the control. CCCP treatment of cells expressing vector alone resulted in a shift from J-aggregate to monomer JC-1 indicating a loss of mitochondrial membrane potential and MMP. In contrast, the J-aggregate to monomer ratio MC163F expressing cells remained unchanged after CCCP treatment.

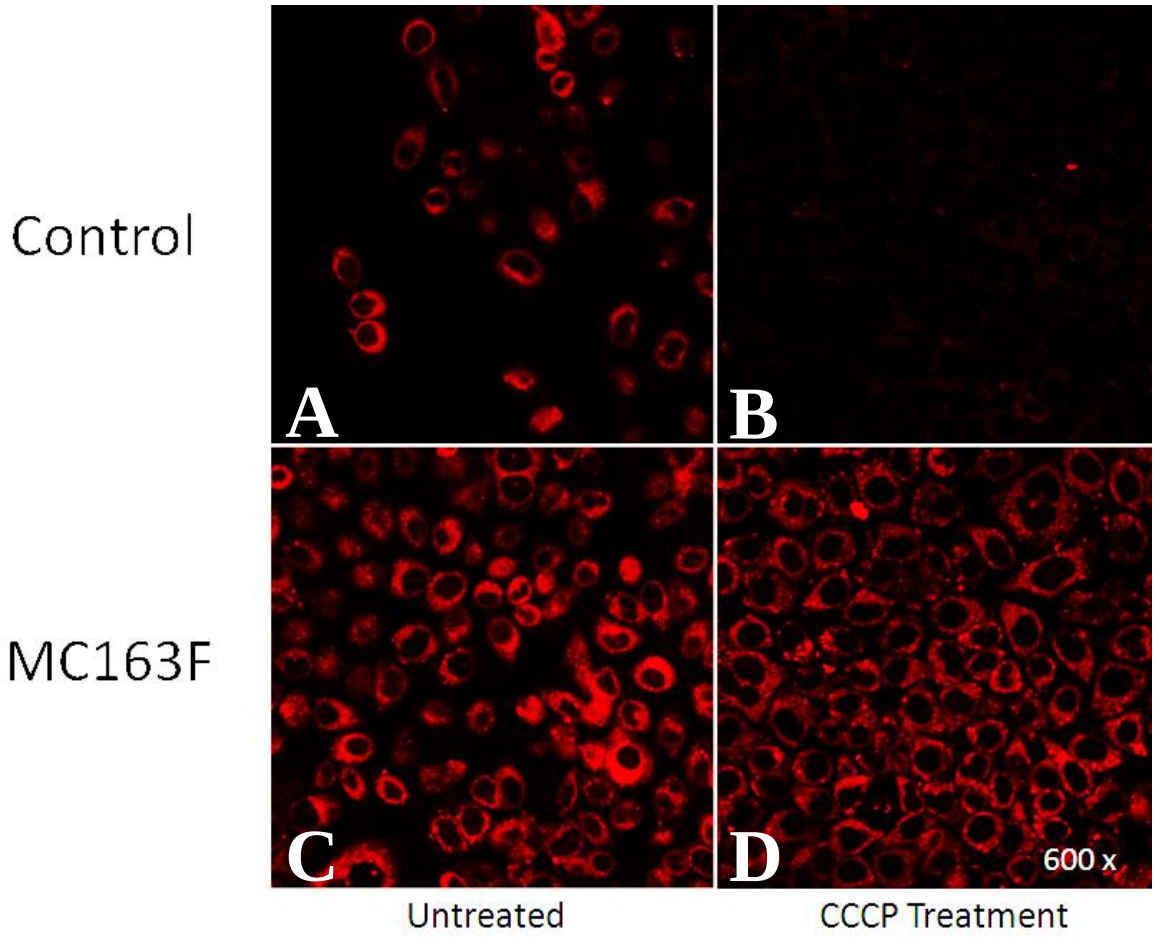

Figure 15: JC-1 staining of HeLa cells treated with and without CCCP (carbonyl cyanide m-chlorophenyl hydrazone). Subconfluent HeLa cells were transfected with pCDNA3.1 (500 ng); pHA-MC159 (500 ng); or pHA-MC163F (500 ng). Twenty four hours later cells were treated with CCCP (100μM/mL) and incubated at 37^{o}C for 30 minutes in a 5% CO_2 humidified incubator. Cells were stained with the cyanine dye JC-1 (5,5′,6,6′-tetrachloro-1,1′,3,3′-tetraethylbenzimi- dazolylcarbocyanine iodide, Cayman Chemical) for 20 minutes then immediately imaged using an Olympus confocal microscope. J-aggregate channel is shown (detection: Ex/Em = 585 nm/590 nm). Untreated cells transfected with pCDNA3.1 (A) and pHA-MC163F (C). Vector control does not block

MMP induced by CCCP treatment (B), however, MC163F does blocks MMP induced by CCCP treatment (D).

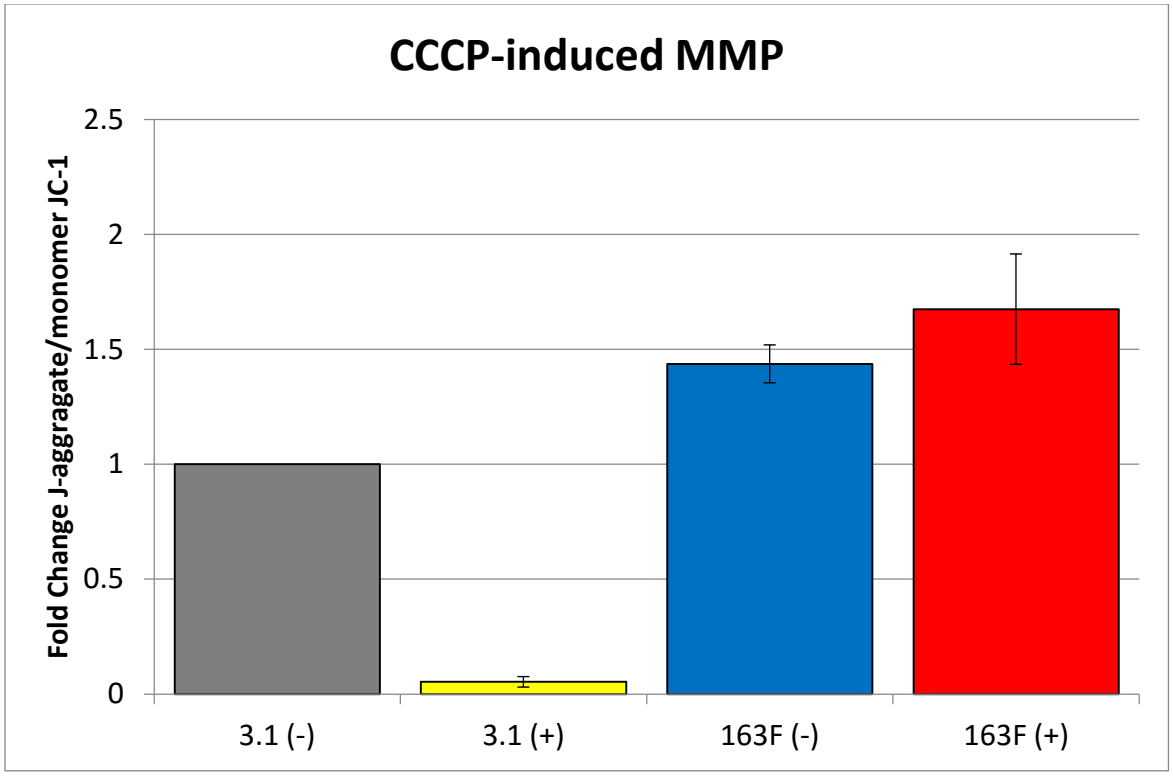

Figure 16: The effect of MC163F on the mitochondrial membrane permeabilization induced by CCCP treatment. Subconfluent HeLa cells were transfected with pCDNA3.1 (500 ng); pHA-MC159 (500 ng); and pHA-MC163F (500 ng). Twenty four hours later cells were treated with CCCP (100μM/mL) and incubated at 37^{o}C for 30 minutes in a 5% CO_2 humidified incubator. Cells were stained with the cyanine dye JC-1 (5,5′,6,6′-tetrachloro-1,1′,3,3′-tetraethylbenzimi- dazolylcarbocyanine iodide, Cayman Chemical) for 20 minutes then immediately imaged using an Olympus confocal microscope (Olympus, Monomer detection: Ex/Em = 514 nm/529 nm, J-aggregate detection: Ex/Em = 585 nm/590 nm). Multiple images were taken for each sample (minimum = 3 images / sample) and analyzed with ImageJ software using the Fiji image processing package (Schindelin, J., et al., 2012). Values represent the ratio of J-aggregate to monomer form

of JC-1 normalized to the control and are shown from one representative experiment, (n=3) as mean +/- standard deviations (SD).

Discussion

In this thesis, we show that MCV contains an MC163R ORF that functions in modulation of apoptosis through modulation of mitochondrial membrane permeabilization (MMP). An N-terminal mitochondrial localization sequence targets MC163R to the mitochondria. The exact mitochondrial location is yet to be determined. MC163R possesses a hydrophobic trans-membrane domain (TMD) flanked by positively charged residues similar to Tom70, a mitochondrial outer membrane protein (Figure 6A). Poxvirus proteins M11L of Myxoma virus and F1L of Vaccinia virus locate to the mitochondria, block apoptosis and contain a similar TMD (Everett et al. 2000; Stewart et al. 2005; Boya et al. 2004). An interesting feature of MC163R is the predicted Copper/Zinc binding domain. This type of domain is typically found in superoxide dismutase proteins. The Myxoma virus protein M131R and Shope fibroma virus S131R proteins modulate apoptosis through inhibition of SOD1 activity by binding to copper chaperone proteins (Teoh et al. 2005). Interestingly, MC163R expressing cells did not exhibit significant changes in SOD1 activity when compared to controls (data not shown).

MC163R mutants were generated after bioinformatics analysis identified protease sites immediately downstream of the TMD (https://prosper.erc.monash.edu.au; calpain-1, GTLY-LIPS, a. a. 180-187; cathespsin K, QVFW-NHSE, a. a. 145-152). The cellular cleavage product of the full length MC163R mutant was identified and can be seen in figure 10A, 50kD band. Both the full length, MC163F and N-terminal MC163N truncated mutants were shown to block TNF-α-induced mitochondrial membrane

permeabilization (MMP) (Figure 13). In contrast, the MC163C mutant loses its ability to block TNF-α-induced MMP (Figure 13). It is not known if the cleavage of MC163R full length is required for its anti-apoptotic function in preventing mitochondrial membrane permeabilization. Additional mutagenesis of these protease cleavage sites may yield clues into the molecular mechanism of MC163R function.

Although The C-terminal domain contains no regions of homology to other proteins it does interestingly contain potential BCL-2 homology (BH) domains (BH1-like domain: a. a. 347-354, 383-399; BH2-like domain, a. a. 558-569; BH3-like domain: a. a. 345-355). Most viral proteins containing BH-like domains are not conserved in the amino acid sequence. However, the viral protein maintains the required structural homology to the cellular BH-containing proteins (Franklin & Khan 2013). The presence of BH-like domains in MC163R might reveal a potential mechanism of function mimicking the anti-apoptotic BcL-2 (Figure 17).

Poxviruses antagonize extrinsic cellular death signaling by competing with receptors for ligands, preventing the activation of caspases, modulating reactive oxygen (ROS) signals and dampening pro-apoptotic signals at the mitochondria (Pogo et al. 2004). MCV contains the death effector domain containing protein, MC159, which blocks apoptotic signals at the death receptor as well as TNF-α-induced MMP (Murao & Shisler 2005; Randall et al. 2012, Struzik et al. 2014; Figure 13). MC163 also blocked TNF-α-induced MMP as shown utilizing the JC-1 stain as an indicator of mitochondrial membrane potential (Figure 13). Whereas, MC159 binds FADD and procaspase-8 at the receptor preventing the formation of the signalsome, the current data suggests MC163

inhibits the extrinsic apoptotic pathway by at the level of the mitochondria, downstream of the activation of caspase 8.

TNF-α is a powerful pro-inflammatory cytokine that activates death pathways as well as the activation of the NF-κB transcription factor which plays a crucial role in the activation of the pro-inflammatory response to viral infection. Viruses have adapted with their host to antagonize the activation of NF-κB at many points within the signal pathway. Two MCV proteins, MC159 and MC160 attenuate NF-κB activation through interaction with the IKK complex, (Nichols & Shisler 2006; Nichols & Shisler 2009; Randall et al. 2012; Struzik et al. 2014). Using a luciferase reporter assay under the control of NF-κB, cells transfected with pHA-MC159 or pHA-MC160 showed a significant reduction in the activation of NF-κB similarly to what has been previously shown (Brady et al., 2015; Murao & Shisler 2005; Randall et al. 2012; Struzik et al. 2014; Nichols & Shisler 2006; Nichols & Shisler 2009). Interestingly, MC163R showed a two-fold decrease in luciferase activity compared to cells transfected with empty vector (Figure 14). Three MCV proteins, so far, have been shown to block NF-κB activation (MC132, MC159, and MC160). Due to the importance in NF-κB signaling in the antiviral response, it makes sense that MCV would have multiple proteins that are capable of attenuating the activation of NF-κB. This work is the first to characterize MC163R and it would be too speculative to make any prediction as to the molecular mechanism of action on NF-κB activation.

Intrinsic activation of apoptosis arises through cellular damage (DNA damage, ER stress) that lead to activation of pro-apoptotic signals converging at the mitochondria.

CCCP is a protonophore that mimics mitochondrial damage and induces MMP and subsequent apoptosis (de Graaf et al. 2004). MC163R blocked CCCP-induced MMP as shown utilizing the JC-1 stain as an indicator of mitochondrial membrane potential (Figure 16). Interestingly, BcL-2 overexpression has also been shown to block CCCP induced MMP, but it not able to prevent $\Delta\psi_m$ (de Graaf et al. 2004). MC163R contains potential BH domains in the uncharacterized C-terminal region making it plausible that MC163R could function to prevent MMP similarly to cBcL-2. Calcium regulation is an important factor in apoptotic signaling. Calcium influx into the mitochondria can cause the opening of the permeability transition pore (Gunter & Sheu 2009). An influx of calcium into the mitochondria signals mitochondrial uncoupling and membrane permeability transition pore (MPTP) opening. Blocking the MPTP opening by Cyclosporin A (CsA) prevents CCCP-induced apoptosis. (Ganote & Armstrong 2003). Interaction of the K7 protein from Kaposi's sarcoma virus has been shown to prevent apoptosis through the binding of the calcium-modulating cyclophilin ligand (CAML) (Feng et al. 2002). Interestingly, the N-terminal MLS and TMD of MC163R has homology to the region in K7 that is responsible for binding CAML (Figure 6C). These data may lead to the discovery of the molecular mechanism for MMP protection by MC163R. It is proposed that MC163 might function in modulating calcium signals at the mitochondria, thus preventing apoptosis (Figure 17).

Future Directions

This work is the first to identify a novel function for the previously uncharacterized MC163 protein as a novel inhibitor of cellular apoptotic responses. MC163R expression likely contributes to MCV pathogenesis by preventing cellular death induced by viral stress during an MCV infection. Experiments are in progress to further confirm the protective effect that MC163 has after stimulation with TNF-α or CCCP. To this end, a fluorescent protein called pBabe-puro-IMS-RP containing the localization sequence of SMAC/Diablo will be utilized (pBabe-puro-IMS-RP was a gift from Peter Sorger (Addgene plasmid # 24535) (Albeck et al. 2008). This protein will localize to the inner-mitochondrial space and upon MMP will dissociate into the cytoplasm. Additionally, experiments are planned to determine the degree that MC163 contributes to MCV pathogenesis using a recombinant vaccinia virus expressing MC163 in a mouse model.

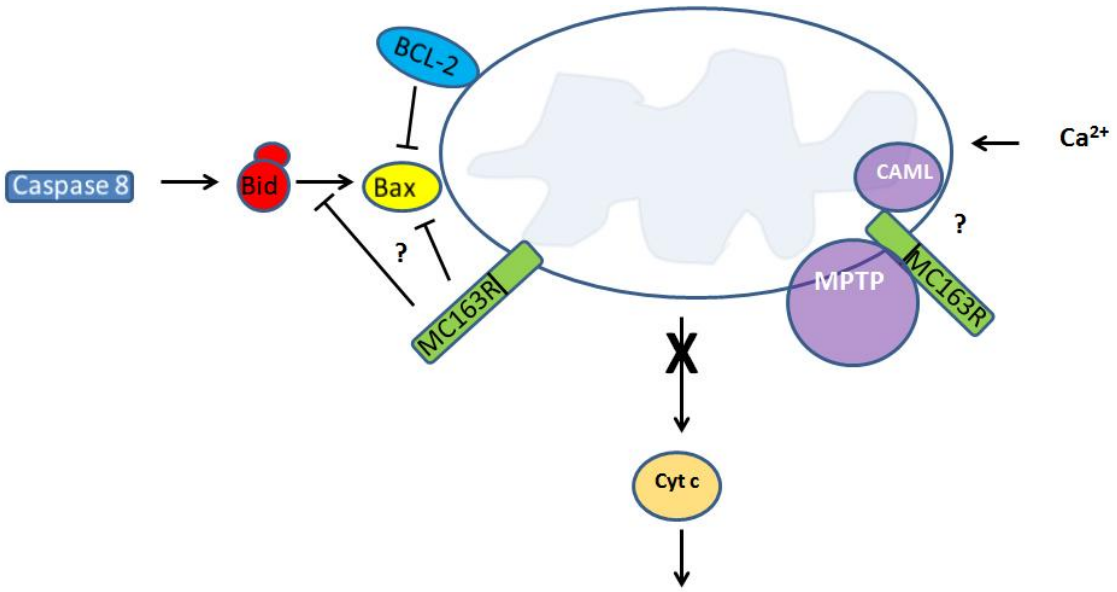

Figure 17: MC163R Model. The MC163 N-terminal region is proposed to modulate calcium-induced apoptosis through the interaction of CAML or the MPTP. BcL-2 homology-like domains in the C-terminal region of MC163 are proposed to interact with pro-apoptotic factors Bax or Bid and help to modulate apoptosis. Bid, BH3 interacting-domain death agonist; Bax, BCL-2 associated X protein; Cyt c, cytochrome c; BcL-2, B-cell lymphoma 2; CAML, calcium-modulating cyclophilin ligand; MPTP, mitochondrial permeability transition pore

References

Alcami, A., Koszinowski, U.H., 2000. Viral mechanisms of immune evasion Molecular mechanisms today, 6: 365-372 PII: S1357-4310(00)01775-5

Amaya, M., Keck, F., Bailey C., Narayanan, A., 2014. The role of the IKK complex in viral infections Pathogens and Disease. 72: 32–44 doi:10.1111/2049-632X.12210

Bahar MW, Graham SC, Chen RA, Cooray S, Smith GL, Stuart DI, Grimes JM. 2011. How vaccinia virus has evolved to subvert the host immune response. J. Struct. Biol. 175:127–134. http://dx.doi.org/10.1016/j.jsb.2011.03.010.

Bannai, H., Tamada, Y., Maruyama, O., Nakai, K., Miyano, S., 2001. Views: Fundamental Building Blocks in the Process of Knowledge Discovery, In Proceedings of the 14th International FLAIRSConference, AAAI Press 233-238

Bannai, H., Tamada, Y., Maruyama, O., Nakai, K., and Miyano, S., 2002. Extensive feature detection of N-terminal protein sorting signals", Bioinformatics, 18:2:298-305

Boya, P., Pauleau, A-L., Poncet, D., Gonzalez-Polo, R-A., Zamzami, N., Kroemer, G., 2004. Viral proteins targeting mitochondria: controlling cell death Biochimica et Biophysica Acta 1659:178– 189

Brady, G., Haas, D.A., Farrell, P.J., Pichlmair, A., Bowiea, A.G., 2015. Poxvirus Protein MC132 from Molluscum Contagiosum Virus Inhibits NF-κB Activation by Targeting p65 for Degradation Journal of Virology 89:16: 8406-8415 doi:10.1128/JVI.00799-15

Bugert JJ, Melquiot N, Kehm R. 2001. Molluscum contagiosum virus expresses late genes in primary human fibroblasts but does not produce infectious progeny. Virus Genes 22:27–33.

Albeck JG, Burke JM, Spencer SL, Lauffenburger DA, Sorger PK., 2008. Modeling a snap-action, variable-delay switch controlling extrinsic cell death. PLoS Biol. 6:12:2831-52. 10.1371/journal.pbio.0060299 PubMed 19053173

Chattopadhyay, S., Marques, J. T., Yamashita, M., Peters, K. L., Smith, K., Desai, A., Williams, B. R.G., Sen, G. C., 2010. Viral apoptosis is induced by IRF-3-mediated activation of Bax The EMBO Journal 29:1762–1773

Chen, Z., J. Hagler, V. J. Palombella, F. Melandri, D. Scherer, D. Ballard, and T. Maniatis. 1995. Signal-induced site-specific phosphorylation targets I kappa B alpha to the ubiquitin-proteasome pathway. Genes Dev. 9:1586–1597.

DiDonato, J. A., M. Hayakawa, D. M. Rothwarf, E. Zandi, and M. Karin. 1997. A cytokine-responsive IkappaB kinase that activates the transcription factor NF-kappaB. Nature 388:548–554.

Elmore S. 2013. Apoptosis: a review of programmed cell death. Toxicol Pathol. 35:495−516.

Emanuelsson, O., Nielsen, H., Brunak, S., von Heijne, G., 2000. Predicting subcellular localization of proteins based on their N-terminal amino acid sequence. J. Mol. Biol., 300:1005-1016

Everett, H., M. Barry, S. F. Lee, X. Sun, K. Graham, J. Stone, R. C. Bleackley, and G. McFadden. 2000. M11L: a novel mitochondria-localized protein of myxoma virus that blocks apoptosis of infected leukocytes. J. Exp. Med. 191:1487–1498.

Feng, P. H., Park, J., Lee, B. S., Lee, S. H., Bram, R. J., Jung, J. U., 2002. Kaposi's sarcoma-associated herpesvirus mitochondrial K7 protein targets a cellular calcium-modulating cyclophilin ligand to modulate intracellular calcium concentration and inhibit apoptosis, Journal of Virology 76 11491– 11504

Franklin, E., Khan, A. R., 2013. Poxvirus antagonism of innate immunity by Bcl-2 fold proteins Journal of Structural Biology 181:1–10

Ganote, C. E., Armstrong, S. C., 2003. Effects of CCCP-induced mitochondrial uncoupling and cyclosporine A on cell volume, cell injury and preconditioning protection of isolated rabbit cardiomyocytes Journal of Molecular and Cellular Cardiology 35:749–759

Goedhart J, von Stetten D, Noirclerc-Savoye M, Lelimousin M, Joosen L, Hink MA, van Weeren L, Gadella TW Jr, Royant A. 2012. Structure-guided evolution of cyan fluorescent proteins towards a quantum yield of 93%. Nat Commun 20;3:751. doi: 10.1038/ncomms1738.

Goedhart, J., von Stetten, D., Noirclerc-Savoye, M., Lemimousin, M., Joosen, L., Hink, MA., van Weeren, L., Gadella, TW. Jr., Royant, A., Structure-guided evolution of cyan fluorescent proteins towards a quantum yield of 93%. Nature Communications, 2012, 1738:1-9

Green, D. R., Llambi, F., 2015. Cell Death Signaling Cold Spring Harb Perspect Biol ;7:a006080

de Graaf, A. O., van den Heuvel, L. P., Dijkmanc, H. B. P. M., De Abreub, R. A., Birkenkampd, K. U., de Wittea, T., van der Reijdena, B. A., Smeitinkb, J. A. M., Jansen,

J. H., 2004. Bcl-2 prevents loss of mitochondria in CCCP-induced apoptosis Experimental Cell Research 299:533– 540

Guan, H., Nuth, M., Zhukovskaya, N., Ling Saw, Y., Bell, E., Isaacs, S.N., Ricciardi, R.P. 2014. A Novel Target and Approach for Identifying Antivirals against Molluscum Contagiosum Virus. Antimicrobial Agents and Chemotherapy 58:12 p. 7383-7389

Gunter, T. E., Sheu, S-S., 2009. Characteristics and Possible Functions of Mitochondrial Ca2+ Transport Mechanisms Biochim Biophys Acta. 1787:11:1291–1308

Haller, S. L., Peng, C., McFadden, G., Rothenburg, S., 2014. Poxviruses and the evolution of host range and virulence Infection, Genetics and Evolution 21:15–40

Huang, Y., Liu, H., Li, S., Tang, Y., Wei, B., Yu, H., Wang, C., 2014. MAVS-MKK7-JNK2 Defines a Novel Apoptotic Signaling Pathway during Viral Infection. PLoS Pathog 10:3: e1004020. doi:10.1371/journal.ppat.1004020

Jin, Q., Altenburg, J.D., Hossain, M.M., & Alkhatib, G. 2011. Role for the conserved N-terminal cysteines in the anti-chemokine activities by the chemokine-like protein MC148R1 encoded by molluscum contagiosum virus. Virology, 417:2:449-456. doi: 10.1016/j.virol.2011.07.001

Kelley, L.A., Mezulis, S., Yates, C.M., Wass, M.N., Sternberg, M.J.E., 2015. The Phyre2 web portal for protein modeling, prediction and analysis Nature Portocols 10:6:845-858

Kiraz, Y., Adan, A., Yandim, M. K., Baran, Y., 2015. Major apoptotic mechanisms and genes involved in apoptosis Tumor Biol. DOI 10.1007/s13277-016-5035-9

Koning S, Bruijnzeels MA, van Suijlekom-Smit LW, van der Wouden JC. 1994. Molluscum contagiosum in Dutch general practice. Br. J. Gen. Pract. 44:386:417–419

Lei Y, Moore CB, Liesman RM, O'Connor BP, Bergstralh DT, Chen, C. J., Pickles, R. J., Ting, J. P. -Y., 2009. MAVS-Mediated Apoptosis and Its Inhibition by Viral Proteins. PLoS ONE 4:5: e5466. doi:10.1371/journal.pone.0005466

Li, H., Lin, X., 2007. Positive and negative signaling components involved in TNF-a-induced NF-kB activation. Cytokine 41:1-8

Luttichau, HR., Gerstoft, J., & Schwartz, T.W. 2001. MC148 encoded by human molluscum contagiosum poxvirus is an antagonist for human but not murine CCR8. Journal of Leukocyte Biology, 70:277-282.

Maadidi, S. E., Faletti, L., Berg, B., Wenzl, C., Wieland, K., Chen, Z. J., Maurer, U., Borner, C., 2014. A Novel Mitochondrial MAVS/Caspase-8 Platform Links RNA Virus-

Induced Innate Antiviral Signaling to Bax/Bak-Independent Apoptosis J Immunol 2014; 192:1171-1183; doi: 10.4049/jimmunol.1300842

Micheau, M., Tschopp, J., 2003. Induction of TNF Receptor I-Mediated Apoptosis via Two Sequential Signaling Complexes Cell, Vol. 114, 181–190

Mohammedamin RS, van der Wouden JC, Koning S 2006. Increasing incidence of skin disorders in children? A comparison between 1987 and 2001. BMC Dermatol. 6:4

Mohr, S., Grandemange, S., Massimi, P., Darai, G., Banks, L., Martinou, J-C., Zeier, M., Muranyi, W., 2008. Targeting the Retinoblastoma Protein by MC007L, Gene Product of the Molluscum Contagiosum Virus: Detection of a Novel Virus-Cell the Molluscum Contagiosum Virus: Detection of a Novel Virus-Cell Journal of Virology 82:21:10625-10633

Murao, L.E., Shisler, J.L., 2005. The MCV MC159 protein inhibits late, but not early, events of TNF-a-induced NF-κB activation Virology 340: 255 – 264 doi:10.1016/j.virol.2005.06.036

Nichols, D.B., Shisler, J.L., 2006. The MC160 Protein Expressed by the Dermatotropic Poxvirus Molluscum Contagiosum Virus Prevents Tumor Necrosis Factor Alpha-Induced

NF-κB Activation via Inhibition of I Kappa Kinase Complex Formation JOURNAL OF VIROLOGY, 80:2:578–586 doi:10.1128/JVI.80.2.578–586.2006

Nichols, D.B., Shisler, J.L., 2009. Poxvirus MC160 Protein Utilizes Multiple Mechanisms To Inhibit NF-κB Activation Mediated via Components of the Tumor Necrosis Factor Receptor 1 Signal Transduction Pathway JOURNAL OF VIROLOGY 83:7:3162–3174 doi:10.1128/JVI.02009-08

Oeckinghaus, A., Ghosh, S., 2009. The NF-κB Family of Transcription Factors and Its Regulation Cold Spring Harb Perspect Biol 1:a000034

Pinton, P., Giorgi, C., Siviero, R., Zecchini, E., Rizzuto, R., 2008. Calcium and apoptosis ER-mitochondria Ca2þ transfer in the control of apoptosis Oncogene 27:6407–6418

Pogo, P. G. T., Melana, S. M., Blaho, J., 2004. Pox virus Infection and Apoptosis International Reviews of Immunology, 23:61–74

http://psort.ims.u-tokyo.ac.jp/

Randall, C. M., Jokela, J. A., & Shisler, J. L. 2012. The MC159 protein from the Molluscum contagiosum poxvirus inhibits NF-kappaB activation by interacting with the IkappaB kinase complex. Journal of Immunology, 188:5:2371–2379

Randall, C. M. H., & Shisler, J. 2013. Molluscum contagiosum virus: Persistence pays off. Future Virology, 8:6:561–573

Randall, C. M., Biswas, S., Selen, C. V., & Shisler, J. L. 2013. Inhibition of interferon gene activation by death effector domain-containing proteins from the molluscum Contagiosum virus. Proceedings of the National Academy of Sciences of the United States of America, 111:2:E265–E272

Rapoport, D. 2003. Finding the right organelle. EMBO Rep. 4:948–952.

Reynolds, M. G., Holman, R. C., Yorita Christensen, K. L., Cheek, J. E., & Damon, I. K. 2009. The Incidence of Molluscum contagiosum among American Indians and Alaska Natives. PLoS One, 4:4:e5255

Roy, A., Kucukural, A., Zhang.T., 2010. I-TASSER: a unified platform for automated protein structure and function prediction. Nature Protocols, 5:725-738

Schindelin, J.; Arganda-Carreras, I. & Frise, E. et al. 2012. "Fiji: an open-source platform for biological-image analysis", *Nature methods* 9:7: 676-682

Scorrano, L., Korsmeyer, J. J., 2003. Mechanisms of cytochrome c release by proapoptotic BCL-2 family members Biochemical and Biophysical Research Communications 304:437–444

Senkevich, T. G., Bugert, J. J., Sisler, J. R., Koonin, E. V., Darai, G., & Moss, B. 1996. Genome sequence of a human tumorigenic poxvirus: Prediction of specific host response-evasion genes. Science, 273:5276:813–816.

Senkevich, T.G., Koonin, E.V., Bugert, J.J., Darai, G., Moss, B., 1997. The Genome of Molluscum Contagiosum Virus: Analysis and comparison with other Poxviruses. Virology 233: 19-42

Sherwani S., Blythe N, Farleigh L, Bugert JJ. 2012. New method for the assessment of molluscum contagiosum virus infectivity. Methods Mol. Biol. 890:135–146.

Shisler, J. L., 2014. Viral and Cellular FLICE-Inhibitory Proteins: a Comparison of Their Roles in Regulating Intrinsic Immune Responses Journal of Virology 88:12:6539–6541 doi:10.1128/JVI.00276-14

Shisler, J. L., Senkevich, T.G., Berry, M.J., & Moss, B. 1998. Ultraviolet-induced cell death blocked by a selenoprotein from a human dermatotropic poxvirus. Science, 279:5347:102–105. doi: 10.1126/science.279.5347.102

Shisler, J. L. 2015. Immune Evasion Strategies of Molluscum Contagiosum Virus. Advances in Virus Research, 92:201-238. doi: 10.1016/bs.aivir.2014.11.004

Shisler, J. L., & Moss, B. 2001. Molluscum Contagiosum Virus Inhibitors of Apoptosis: The MC159 v-FLIP Protein Blocks Fas-Induced Activation of Procaspases and Degradation of the Related MC160 Protein. Virology, 282:1:14-25. doi:10.1006/viro.2001.0834

Smith GL, Benfield CT, Maluquer de Motes C, Mazzon M, Ember SW, Ferguson BJ, Sumner RP. 2013. Vaccinia virus immune evasion: mechanisms, virulence and immunogenicity. J. Gen. Virol. 94:2367–2392. http://dx.doi.org/10.1099/vir.0.055921-0

Stewart, T. L., S. T. Wasilenko, and M. Barry. 2005. Vaccinia virus F1L protein is a tail-anchored protein that functions at the mitochondria to inhibit apoptosis. J. Virol. 79:1084–1098.

Struzik, J., Szulc-Dąbrowska, L., Niemiałtowski, M., 2014. Modulation of NF-κB transcription factor activation by Molluscum contagiosum virus proteins Postepy Hig Med Dosw (online), 68:129-136 e-ISSN 1732-2693

Teoh, M. L. T., Turner, P. V., Evans, D. H., 2005. Tumorigenic Poxviruses Up-Regulate Intracellular Superoxide To Inhibit Apoptosis and Promote Cell Proliferation Journal of Virology, 79:9:5799–5811 doi:10.1128/JVI.79.9.5799–5811.2005

Thome, M., Schneider, P., Hofmann, K., Fickenscher, H., Meinl, E., Neipel, F., Mattmann, C., Burns, K., Bodmer, J.L., Schröter, M., Scaffidi, C., Krammer, P.H., Peter, M.E., & Tschopp, J. 1997. Viral FLICE-inhibitory proteins (FLIPs) prevent apoptosis induced by death receptors. Nature, 386:6624:517-521. doi:10.1038/386517a0

http://www.ch.embnet.org/software/TMPRED_form.html

Tyring SK. 2003. Molluscum contagiosum: the importance of early diagnosis and treatment. Am. J. Obstet. Gynecol.189:3 Suppl.:S12–S16

Upreti, M., Chu, R., Galitovskaya, E., Smart, S. K., Chambers, T. C., 2008. Key role for Bak activation and Bak-Bax interaction in the apoptotic response to vinblastine Mol Cancer Ther. July ; 7:7:2224–2232. doi:10.1158/1535-7163.MCT-07-2299

Xiang, Y., Moss, B. 2003. Molluscum contagiosum virus interleukin-18 (IL-18) binding protein is secreted as a full-length form that binds cell surface glycosaminoglycans through the C-terminal tail and a furin-cleaved form with only the IL-18 binding domain. Journal of Virology, 77:4:2623-2630. doi: 10.1128/JVI.77.4.2623-2630.2003

Yang, J., Yan, R., Roy, A., Xu, D., Poisson, J., Zhang. Y., 2015. The I-TASSER Suite: Protein structure and function prediction. Nature Methods, 12: 7-8

Yuan, S., Akey, C. W., 2013. Apoptosome structure, assembly and procaspase activation Structure. April 2; 21:4:501–515. doi:10.1016/j.str.2013.02.024.

Yu Lei, Y., Moore, C. B., Liesman, R. M., O'Connor, B. P., Bergstralh1, D. T., Chen, Z. J., Pickles, R. J., Ting, R. P. Y., 2009. MAVS-Mediated Apoptosis and Its Inhibition by Viral Proteins PloS One 4:5:1-12

Zhang, Y., 2008. I-TASSER server for protein 3D structure prediction. BMC Bioinformatics, 9: 40.